Nanoscale Horizons

REVIEW

View Article Online
View Journal | View Issue

Cite this: *Nanoscale Horiz.*, 2023, **8**, 1485

A cooperation tale of biomolecules and nanomaterials in nanoscale chiral sensing and separation

Tingting Hong, *[a] Wenhu Zhou, [bc] Songwen Tan[bd] and Zhiqiang Cai *[ad]

The cooperative relationship between biomolecules and nanomaterials makes up a beautiful tale about nanoscale chiral sensing and separation. Biomolecules are considered a fabulous chirality 'donor' to develop chiral sensors and separation systems. Nature has endowed biomolecules with mysterious chirality. Various nanomaterials with specific physicochemical attributes can realize the transmission and amplification of this chirality. We focus on highlighting the advantages of combining biomolecules and nanomaterials in nanoscale chirality. To enhance the sensors' detection sensitivity, novel cooperation approaches between nanomaterials and biomolecules have attracted tremendous attention. Moreover, innovative biomolecule-based nanocomposites possess great importance in developing chiral separation systems with improved assay performance. This review describes the formation of a network based on nanomaterials and biomolecules mainly including DNA, proteins, peptides, amino acids, and polysaccharides. We hope this tale will record the perpetual relation between biomolecules and nanomaterials in nanoscale chirality.

Received 7th April 2023,
Accepted 17th August 2023

DOI: 10.1039/d3nh00133d

rsc.li/nanoscale-horizons

[a] School of Pharmacy, Changzhou University, Changzhou, Jiangsu 213164, China. E-mail: zhqcai@cczu.edu.cn, hongtingting0203@163.com
[b] Xiangya School of Pharmaceutical Sciences, Central South University, 172 Tongzipo Road, Changsha, Hunan 410013, China
[c] Academician Workstation, Changsha Medical University, Changsha 410219, China
[d] Jiangsu Dawning Pharmaceutical Co., Ltd, Changzhou, Jiangsu 213100, China

1. Introduction

There exist all sorts of beautiful relations in a temporal and spatial context. Herein, a cooperation tale of biomolecules and nanomaterials (NMs) in nanoscale chiral sensing and separation is shared. If a cooperation fellowship is developed,

Tingting Hong

Tingting Hong obtained her PhD degree from China Pharmaceutical University in 2017. In 2016–2017, she worked as a CSC joint-PhD student at Vrije Universiteit Brussel. In 2018–2020, she was a postdoc with the research mainly focusing on the application of capillary electrophoresis for separation science at Central South University. She is currently a teacher at Changzhou University. She has published several papers on chiral separation, capillary electrophoresis, and nanomaterials in Analytical chemistry, Journal of Chromatography A, Talanta, Analytica Chimica Acta, Analyst, Analytical Bioanalytical Chemistry, Electrophoresis, Journal of Separation Science, Analytical Biochemistry, and Trends in Analytical Chemistry.

Wenhu Zhou

Wenhu Zhou obtained his PhD degree from Central South University in 2016. From 2014 to 2016, he worked as a CSC joint-PhD student at the University of Waterloo. He is currently a professor at Central South University. He has published several papers on functional nucleic acids, bioanalysis, capillary electrophoresis, nanomaterials, biomedicine, pharmaceutics, and cancer therapy in Nanoscale, Analytical chemistry, Analyst, Nano Letters, ACS Applied Materials & Interfaces, Acta Biomaterialia, Microchimica Acta, Analytica Chimica Acta, etc.

biomolecules and NMs shall become valuable to each other. This win–win cooperation enables the integration of their advantages, unlocking the potential of biomolecules and NMs. We envision that such 'backscratching' tenant will sustain the relationship forever.

As one of the predominant attributes of nature, chirality is omnipresent at multiple scales, ranging from subatoms to galaxies.[1–5] Homochirality might be linked to the origin of life. The term chiral stems from the Greek word for hand *χείρ*. Chirality refers to a geometric trait of structures, and a chiral structure cannot be superimposed on its mirror image *via* the geometrical transformations. These configurations of opposite handedness are called enantiomers. In an achiral environment, chiral enantiomers share physical and chemical properties, and the two enantiomers can be considered as one substance. Nevertheless, the enantiomers usually present different biological and pharmacological activities in a chiral organism. Due to the specific chiral recognition capability of natural biomolecules toward enantiomers, the organism displays a special interaction mechanism in versatile biological events, and chiral recognition has an essential role in human life. Moreover, biomolecules are endogenous chiral selectors with a wide variety, which can avoid the complicated reaction steps required for preparing other artificial chiral selectors. Consequently, the close relationship between biomolecules and chiral applications makes natural biomolecules a desirable candidate for enantiomeric sensing and separation.

For millions of years, biological species have been constantly evolving to realize their admirable biofunctionalities. The integration of NMs with biological systems is considered an intriguing alternative for augmenting the functions of natural biosystems. Meanwhile, biological elements extensively contribute to the renewed vitality of nanotechnology.[6–13] Nanotechnology was first introduced to the world by Nobel laureate Richard P. Feynman in his famous speech 'There is Plenty of Room at the Bottom'. Soon afterward, the field of NMs started taking off. To achieve the exquisite control of components motion on the nanoscale is an ambitious goal in nanotechnology. Self-assembly, the spontaneous organization of basic units into ordered structures utilizing noncovalent interactions, creates versatile configurations in nature.[14–18] Nature possesses prominent competence to assemble biomolecules at near-atomic precision. Nevertheless, we are nowhere near the limit of exquisite control over life. DNA is a beautiful example of the natural self-assembling biomolecules. The information encoded in DNA facilitates the assembling of one DNA strand with its complement based on extremely precise Watson–Crick base pairing, thus outlining a genetic blueprint for life. Owing to the high predictability and programmability of oligonucleotides, DNA provides a favorable scaffold for nanoscale fabrication.[19–25] A nearly infinite amount of sequences enable synthetic DNA nanostructures to far surpass what nature has constructed with DNA. DNA technology has been revolutionary in our ability to regulate molecular self-assembly. An event is an effect beyond a cause. Before the inception of DNA nanotechnology, we could never have imagined establishing such complicated structures. Since programmable DNA and peptide sequences enable the controllability of building blocks position at the nanometer level, biomolecules such as DNA, proteins, peptides, and amino acids (AAs) have emerged as desirable alternatives for controlling the chiral structure of NMs.[26–31] Moreover, polysaccharides possessing multiple chiral identification sites exhibit desirable enantiorecognition ability as well.[32,33] A harmonious relationship between biomolecules and nanotechnology has been created in chiral sensing. Combining biomolecules and NM into 'smart' hybrid configurations has attracted widespread attention in natural and materials sciences. The incomparable nanocomposites integrate biomolecules chirality and the satisfactory optical, electrical, and thermal characteristics of NMs. 'Chiral transfer' can be realized by imparting biomolecules chirality to achiral NMs. The cooperation of biomolecules and NMs in chiral sensing facilitates signal amplification and sensitivity enhancement. Biomolecules include DNA,

Songwen Tan

Songwen Tan obtained his PhD degree from University of Sydney in 2019. He is currently a professor at Central South University. He has published several papers on capillary electrophoresis, bioanalysis, nanomaterials, pharmaceutics, environment and food analysis in Analytical chemistry, Analyst, Talanta, Trends Food Sci Technol, Food Hydrocoll, Chemosphere, Powder Technology, Materials & Design, Energy, Environmental Toxicology and Pharmacology, Bioresource Technology, Biotechnology Letters, etc.

Zhiqiang Cai

Zhiqiang Cai obtained his PhD degree from Zhejiang University. Zhiqiang Cai is currently a professor at School of Pharmacy, Changzhou University. Professor Cai's research interests include biotechnology, biocatalysis, capillary electrophoresis, nanomaterials, and fermentation engineering with several publications in Analytical Chemistry, Nanomaterials, Biosensors and Bioelectronics, Analyst, Journal of Agricultural and Food Chemistry, etc.

proteins, peptides, AAs, and polysaccharides—what gives them their beauty is something that is invisible to the eye. This sightless chirality can be discovered and appreciated using our 'heart': NMs.

Considering their tremendous merits, biomolecules-based chiral sensors have been a topic of keen interest in a wide field of applications. It provides a predominant inspiration to integrate biomolecules and NMs in chiral separation to see what will happen when two elements meet. Among a variety of analytical enantioselective approaches, capillary electrophoresis (CE) has been attracting attention for chiral separation, with miniaturization becoming a trend in separation science.[34–37] Enantioseparation benefits from the attractive advantages of CE include its fast analysis speed, high resolution efficiency, and low reagent consumption. Developing innovative chiral selectors has occupied a crucial position in chiral CE.[38,39] NMs with large surface area are favorable carriers for enhancing biomolecules immobilization efficiency on capillaries and improving enantioseparation performance in terms of selectivity and efficiency.[40,41] The cooperation of biomolecules and NMs has paramount importance in fabricating enantiomeric separation systems.

We showcase a cooperation tale of biomolecules and NMs in nanoscale chiral sensing and separation (Scheme 1). Scientists' innovative ideas have made great contributions to the exploitation of chirality. The cooperation between NMs and biomolecules is helpful in speeding up the development of nanoscale chirality. Biomolecules can cooperate with NMs to form an amazing network, making them broader than themselves. This relation organizes individual matters into a meaningful whole for chiral sensing and separation. We highlight the state-of-the-art studies in which biomolecules-based nanoscale chirality gives rise to large-scale scientific endeavors. Chiral biological macromolecules and achiral NMs are important in constructing chiral plasmonic NMs. Circular dichroism (CD) responses of chiral plasmonic nanostructures display promising potential for chiral sensing. Various approaches applied to fabricate chiral plasmonic systems will be discussed in detail. Moreover, we will review the advances in electrochemical, fluorescent, and colorimetric sensors employed as analytical platforms for chiral sensing research. The prospect of utilizing the unique properties of NMs for developing biomolecules-based chiral CE separation systems will be further summarized. We hope the decoration in chiral sensors is able to spur the advancement of biomolecule-NMs cooperation in chiral separation. The advantages of combining NMs and biomolecules such as DNA, proteins, peptides, AAs, and polysaccharides will be described in this article. We envision that the cooperation of NMs with biomolecules will open up new avenues in nanoscale chiral sensing and separation.

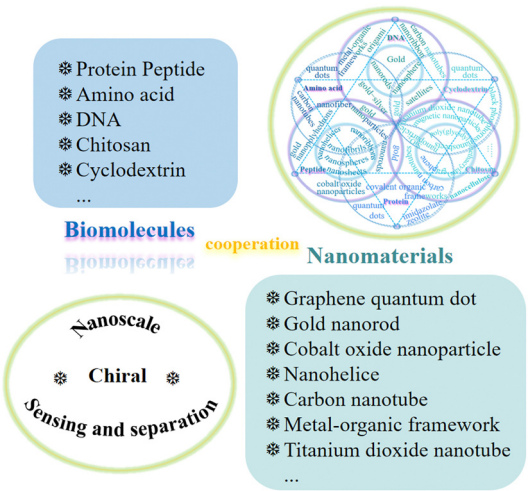

Scheme 1 The cooperation of biomolecules and nanomaterials in nanoscale chiral sensing and separation.

2. A cooperation tale of biomolecules and nanomaterials in chiral sensing

The cooperation of biomolecules with NMs provides a marvellous opportunity for developing miniaturized chiral sensors. Chiral biomolecules such as DNA, protein, and polysaccharide are able to construct the basic molecular units of life. The chiral information encoded in biomolecules plays an important role in molecular recognition. Therefore, the inherent chirality of biomolecules makes them a desirable enantiomer selector.[42–44] Increasing attention has been paid to NMs depending on their desirable optical, electrical, and thermal properties.[45–48] Integrating these specific characteristics of biomolecules and NMs is the key point in chiral sensing. The obtained sensors facilitate the transfer of biomolecules chirality, amplification of chiral signal, and improvement of sensitivity. Various types of biomolecules and NMs are reviewed in this article. The cooperative relationship between biomolecules and NMs for fabricating chiral sensors can be classified into three groups: bio-NMs, biomolecule-NM, and biomolecule-like NMs.

2.1. Creating a cooperative relationship between DNA and nanomaterials in chiral sensing

DNA nanotechnology has emerged as an efficient technique in biosensors development using DNA as a construction element for assembling nanostructures. The design of chiral plasmonic NMs has received considerable interest owing to their potential applications in various domains such as material science, medicine, and nanotechnology.[49–51] DNA nanotechnology provided efficient approaches for designing chiral templates of different geometries. To fabricate desirable chiral plasmonic systems, nanostructures synthesized by the self-assembly of DNA have been efficiently employed as templates. The spatial addressability of DNA NMs facilitated the preparation of extremely complicated plasmonic systems. Much efforts have been focused on investigating simple and favorable strategies for the development of DNA-based chiral templates.

Since the combination of biological molecules and metal nanoparticles (NPs) plasmonic feature enables the amplification of chiral information, regulating the biomolecules'

plasmonic CD occupies an essential position in chiral sensing. CD is an absorption spectroscopy approach depending on the differential absorption of right and left circularly polarized light. Optically active chiral molecules preferentially absorb one direction of the circularly polarized light. The difference in the absorption of the right and left circularly polarized light can be measured. Among different DNA NMs, DNA origami is beneficial for the design of complicated NMs by integrating multiple functional constituents with nanometer precision.[52–55] The configurability of DNA origami structures permits the achievement of tailoring biosensors. Metal NMs have been considered desirable optical transducers for sensing. Depending on 'DNA origami' technology, metal NMs can be assembled onto specific binding sites for producing complicated configurations with nanoscale precision. In addition, the intrinsic dynamics of DNA facilitates the modulation of the template conformational changes and control of the chiral signal. Reconfigurable chiral plasmonic systems assembled by DNA present tremendous advantages in sensing applications since CD spectroscopy can be used to reflect their structural information.[56,57] The inherent sequence and site addressability of DNA origami structures facilitated the development of templates for chiral molecules precisely placed in the plasmonic hotspot.[58] DNA origami technology provided an efficient strategy for assembling chiral transfer structures with high precision and yields. Liedl *et al.* prepared a compound DNA origami platform utilizing thiol DNA functionalization and specific handle strands, accommodating two gold nanorods (GNRs) at its ends (Fig. 1(a)). The NRs possessed a surface-to-surface distance of 62 nm, and an L-shaped object was found due to the overlapping of NRs when observing along the origami structure axis. Plasmon-assisted chiral interactions occurred in the chiral assemblies of two NRs. Moreover, a gold nanosphere (NS) was attached in between a pair of NRs. The influence of an achiral NS in a chiral structure based on DNA origami was explored. This spherical transmitter particle was able to couple the chirality response of the rods, causing a strong signal improvement of the CD response. The proposed nanostructures could be potentially employed as a novel type of chiral sensors for biomolecules. A DNA origami-based chiral plasmonic sensor was employed for detecting RNA at 100 pM by choosing DNA-based molecular 'lock' as a biorecognition component.[59] Chiral plasmonic NMs possessing strong chiroptical signals facilitated asymmetric photophysical and photochemical processes utilizing circularly polarized light. Govorov *et al.* applied the photothermal chirality properties of plasmonic NMs for the asymmetric DNA origami melting.[60] As seen in Fig. 1(b), the proposed structure is a chiral assembly composed of two rotated GNRs bounding *via* DNA origami (purple block). A dimer with $\emptyset = 45^\circ$ is called the L-pair, exhibiting maximum left-handedness. The chiral photothermal effect could selectively melt the DNA linker strands. Compared with the chiral molecular photochemistry, the asymmetry factors of the designed plasmonic photosystems improved at least 10-fold. The results indicated that the plasmonic nanostructures provided an efficient platform for investigating chiral photophysical effects and enantioseparation at the nanoscale.

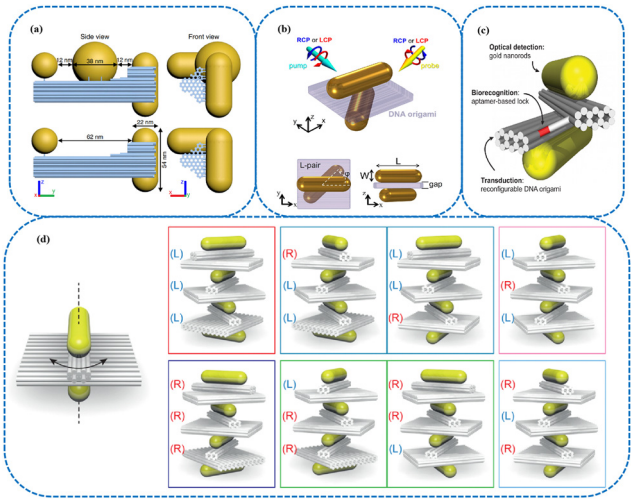

Fig. 1 (a) Side view and front view of DNA origami-nanoparticle assemblies in a nanorod–nanosphere–nanorod arrangement, and a nanorod–void–nanorod arrangement. The nanorods and the nanosphere are mounted on a DNA origami structure (blue cylinders represent DNA helices) *via* thiolated DNA strands that are anchored to the origami structure.[58] Reprinted from K. Martens *et al.*, *Nat. Commun.*, 2021, **12**, 2025 Copyright (2021), with permission from Springer Nature. (b) Schematics of the rotated gold dimer upon CP illumination and CP probe (cyan and yellow beams, respectively, with either red or blue circular polarized light CPL) with panoramic view (top panel) and top and side views (bottom panels).[60] Reprinted from O. Ávalos-Ovando *et al.*, *Nano Lett.*, 2021, **21**, 7298–7308 Copyright (2021), with permission from American Chemical Society. (c) Schematics of the DNA origami-based chiral plasmonic nanosensor. The DNA aptamer-based molecular lock is employed as a biorecognition element incorporated into a reconfigurable DNA origami structure, which hosts two GNRs. Two GNRs constitute a three-dimensional (3D) chiral plasmonic object with circular dichroism optical response, which is dependent on the angle between the rods.[68] Reprinted from Y. Huang *et al.*, *ACS Appl. Mater. Interfaces*, 2018, **10**, 44221–44225 Copyright (2018), with permission from American Chemical Society. (d) DNA origami templates are used for the assembly of gold nanorods (GNRs). The configuration of origami-GNR constructs can be actively switched between right- and left-handed chiral configurations. Four GNRs and three DNA origami constructs are used for the assembly of plasmonic structures with three chiral centers, which give rise to eight origami-nanorod stereoisomers and six unique chiral plasmonic spatial configurations.[64] Reprinted from M. Nguyen *et al.*, *ACS Nano*, 2019, **13**, 13615–13619 Copyright (2019), with permission from American Chemical Society.

In addition, giant g-factors observed in the referenced study suggested the promising potential of this system for chiral photoreactions. To adapt to environmental changes, living cells can regulate macromolecules geometrical variations and realize particular biofunctions. Consequently, efforts have been made to develop artificial macromolecules possessing adjustable nanostructures and environmentally responsive features. DNA origami was used as a template for assembling L-shaped GNRs.[61] The resulting chiral plasmonic sensor could transfer external stimuli to geometrical changes and CD chiral signal responses. Many efforts have been focused on exploring strategies to impart the spatial information of DNA origami to metal NMs. Shen *et al.* developed a DNA-assisted lithography approach by combining the robustness of traditional

lithography technologies and the structural diversity of DNA origami.[62] To explore the relationships between chiral geometry and the physical characteristics of chiral materials has become a focus of attention in the chiral amplification process.[63] In addition to plasmonic enantiomers, architectures with up to three chiral centers were designed depending on the multiple chiral centers concept in stereochemistry.[64] To investigate the DNA origami-based assembly of plasmonic structures, DNA origami containing a two-layer rectangular plate and 10-helix bundle was utilized as templates for hosting GNRs (Fig. 1(d)). The NRs could be switched between the right- and left-handed chiral configurations *via* toehold-mediated DNA strand displacement reactions. Furthermore, up to four GNRs were able to be linked together with DNA origamis. Each pair of neighboring GNRs were regarded as a chiral center. This proposed system with controllable multiple chiral centers provided a promising platform for the simultaneous detection of multiple targets. As we know, gold NPs (GNPs) have been widely used owing to their high chemical stability. Nevertheless, silver NPs possess better optical characteristics. Innovative DNA origami-coated GNR/AgNRs were synthesized *via* a simple one-pot reaction.[65] This bimetallic plasmonic system presented enhanced CD responses compared with its Au counterpart. The results suggested that gold–silver NRs were desirable candidates for achieving increased sensitivity due to their cooperative and synergistic effects. The respective localized surface plasmon resonance was able to be tuned, and the biocompatibility of these bimetallic particles was further improved by conjugating with DNA. DNA origami could also be incorporated with achiral biscyanine dyes to prepare circularly polarized luminescence (CPL) active materials.[66,67] CPL reflected the differential emission of right- and left-handed CP light from chiral emitters. The chirality of the DNA molecules was transferred to the achiral cyanine molecules, triggering remarkable CPL emission. Moreover, the structures of DNA templates were able to regulate the chirality of the CPL signal. This work provided an efficient pathway to develop different DNA NMs for CPL-based chiral sensing.

The optical responses of chiral plasmonic nanostructures facilitated the construction of aptamer-based sensing platforms as well. Huang *et al.* designed DNA origami-based chiral nanosensor by combining the advantages of aptamers, DNA origami, and chiral plasmonics (Fig. 1c).[68] Aptamers were favorable biorecognition elements to be integrated into DNA origami configuration owing to their high affinity and specificity toward various target molecules.[69–72] Two 14-helix bundles were linked in the center of DNA origami, and the orientation of the bundles could induce right- or left-handed spatial structure. To achieve optical detection of the chiral nanostructures, two GNRs were assembled on top of the DNA origami. The optical responses could be optimized by the size and material composition of the NRs. Results indicated that the proposed nanoscale sensor exhibited high selectivity and sensitivity for detecting targets in strongly absorbing fluids, thus simplifying the sample preparation procedures. Dynamic DNA origami configuration was able to be adjusted according to the specific targets. The programmability of this assembly facilitated the incorporation of biorecognition elements at suitable locations. Due to their delicate and structurally well-defined properties, self-assembled nanosuperstructures have attracted increasing interest nowadays. A nanosuperstructure with a high CD signal was beneficial for improving the detection sensitivity of biological samples. Kuang *et al.* constructed an aptamer-based chiral biosensor for ochratoxin A (OTA) detection.[73] The resulting shell core-gold satellite sensor displayed an obvious signal with a strong CD peak. This chiral intensity could be weakened correspondingly with the increased OTA contents. Therefore, OTA concentrations were able to be determined according to the impaired chiral signal. Generally, specific interaction between structured nucleic acids and enantiomers facilitated the development of clinically chiral drugs. Aside from aptamer, G-quadruplexes (G4s) provided desirable chiral platforms since their polymorphism structures could adjust their stereoselective binding with different isomers.[74] Exploring the recognition mechanism of DNA and chiral substances was important for designing DNA-based sensors. L-DNA was the mirror-image counterpart of natural DNA. G4 DNA with diverse configurations and distinctive biofunctions were chosen to evaluate the binding mechanisms of iron triplex metallohelices to enantiomeric G4.[75]

In addition to DNA origami, DNA-based nanoribbons derived from the self-assembly of ssDNA and hexaphenylbenzene (HPB) were exploited for developing chiral plasmonic nanostructures (Fig. 2(A)).[76] The ribbons were obtained depending on the hydrophobic interactions of HPB. Although the obtained NMs presented limited structural diversity, the

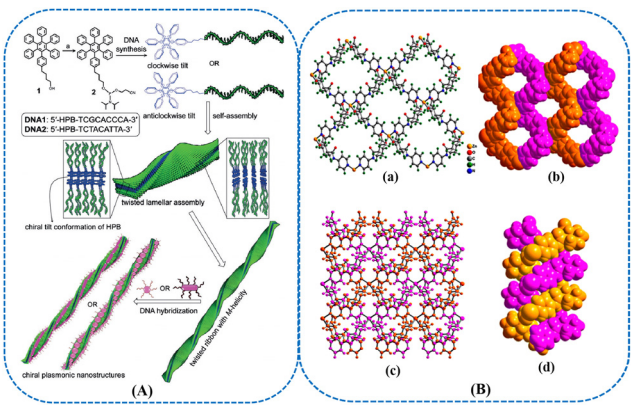

Fig. 2 (A) Synthesis of DNA-based amphiphiles through phosphoramidite chemistry. Conditions: (a) CH_2Cl_2, diisopropylamine, 2-cyanoethyl-*N*,*N*-diisopropylchlorophosphoramidite, RT, 2 h, 80%. Schematic for the self-assembly of DNA-based amphiphiles into DNA-decorated, twisted nanoribbons with M-helicity. DNA-directed chiral organization of AuNPs and AuNRs is also shown.[76] Reprinted from M. Golla *et al.*, *Angew. Chem. Int. Ed.*, 2019, **58**, 3865–3869 Copyright (2019), with permission from Wiley. (B) (a) Ball and stick view of a single 2D layer of HMOF-1. (b) Space-filling view of a single 2D layer showing right-handed 2-fold helical chains along the *b*-axis. (c) 2-fold interpenetrated layers. (d) Space-filling view of right-handed double helix.[87] Reprinted from Y. W. Zhao *et al.*, *ACS Appl. Mater. Interfaces*, 2017, **9**, 20991–20999 Copyright (2017), with permission from American Chemical Society.

design and synthesis process for DNA-based amphiphile self-assembly was simple. Moreover, this strategy facilitated the introduction of hydrophobic elements into the DNA nanostructures. The transformation of DNA chirality into the HPB enabled the bias of one of the chiral propeller conformations for HPB, resulting in the formation of nanoribbons with left-handed helicity. Furthermore, DNA-based chiral nanoribbons were applied as universal templates for fabricating chiral plasmonic systems by the assembly of GNPs or GNRs. These formed chiral nanostructures with one handedness possessed a promising potential in chiral sensing. The DNA adaptors could be programmably connected into distinct stair-like or coil-like chiral supramolecular architectures with tuned handedness.[77] Such supramolecular assembly of DNA adaptor was able to be applied to govern the tunable directional self-assembly of GNRs decorated by the DNA adapter. The spatial arrangement of the NR pair could give rise to the different optical chirality of the ensemble conformation. Chirality and induced superhelicity in living organisms have attracted intense attention. In addition to DNA, RNA was utilized to prepare the supramolecular architectures as well. Owing to their reliable base pairing and satisfactory stability, nucleic acids were considered desirable templates for the precise arrangement of molecular components into supramolecular nanoassemblies. The homochiral ssRNA could be used as templates to develop chiral double-zipper supramolecular nanostructures.[78] We believe that more work should be focused on investigating RNA-based NMs for chiral sensing. DNA, possessing double-stranded helical conformation, was considered a prominent 'building block' biomolecule.[79] As the vector of genetic information, DNA possesses intrinsic chirality. The chirality of some enantiomers has a great influence on their bioactivities. It is difficult to separate and monitor enantiomers due to their identical physical and chemical features. The programmable self-assembly of DNA has been widely utilized to build novel metallic NMs-based sensors with controllable optical properties.

As a type of crystalline porous material, metal–organic frameworks (MOFs) have drawn increasing interest nowadays.[80–84] AAs possess two steric configurations, and the L-form usually exists in the organism and nature.[85,86] The appearance of the D-form can suggest a negative symptom or disease. Therefore, designing a chiral sensor for AAs detection is important in diseases diagnosis. As we know, CD is able to display the absolute molecular configuration of enantiomers. It is necessary to develop a simple CD approach for sensing AAs without complicated chemical reaction. A chiral MOF-based sensor was constructed for recognizing unmodified AA.[87] This homochiral MOF (HMOF-1) possessing right-handed double-helix conformation was assembled by zinc salt and chiral ligand (Fig. 2(B)). The DNA-like HMOF-1 presented inherent CD signal, and the intensity of this signal was able to be changed by the interaction between AAs and MOF. The results indicated that the interacting mechanism of HMOF-1 with AAs was similar to that of the groove binding of molecules with DNA. The resulting chemosensor exhibited tremendous advantages for the sensitive and rapid detection of micro amounts of AAs.

Compared with traditional ferromagnets, DNA was referred to as a spin filter with better 'chirality-induced spin selectivity' effect. Owing to their intrinsic helicity, DNA were able to wrap carbon nanotubes (CNTs) in a helical morphology. Since longer nanotubes-DNA were proposed to produce higher spin polarization degree, long CNTs ($\sim$1–4 μm) were wrapped with DNA for applying as a desirable source and detector of spin-polarized carriers.[88] The resulting CNTs-DNA system presented specific advantages in the area of chiral spintronics. Single-walled CNTs (SWNTs) and DNA hybrids could form stable hybrids based on their complementary structural properties. Since the recognition ability of DNA toward SWNTs was related to the relationship between the specific bases of DNA sequences and the chirality of SWNTs, exploiting the interaction mode between the SWNT and DNA sequence was essential for DNA–SWNT hybrid applications. An electrochemical approach was utilized for investigating the interaction between DNA and two types of chiral SWNTs.[89] Results suggested that the DNA length and sequence composition played a crucial role in the chirality selection progress of DNA and SWNTs. The proposed DNA–CNT hybrids could be considered a potential alternative for developing chiral sensors.

A variety of NMs can be employed for constructing state-of-the-art chiral sensors by choosing DNA as a chiral support. DNA nanostructures such as DNA origami and nanoribbons exhibit substantial benefits in the development of chiral plasmonic systems. This cooperative relationship between DNA and NMs facilitates the formation of tailoring sensors with nanometer precision. Furthermore, the cooperation between DNA chirality and metal NMs plasmonic property enables the amplification of signals. Different types of metal NMs, including GNRs, gold NSs, GNPs, and gold–silver NRs have been used for fabricating chiral sensors with desirable sensitivity. The broad application of chiral plasmonic systems promotes interest in exploring DNA such as NMs. This innovative cooperation approach between DNA and HMOF-1 is described. In addition to metal NMs, the advantages of combining CNTs with DNA are reviewed in this section.

2.2. Creating a cooperative relationship between proteins and nanomaterials in chiral sensing

Proteins have been considered a satisfactory alternative for chiral sensing owing to their stereoselective characteristics.[90,91] 'Chiral transfer' strategy facilitates the simple preparation of protein-based sensors by imparting chirality from chiral proteins to achiral NMs. Based on the prominent advantages of NMs, protein–NM complexes can be utilized for fabricating chiral electrochemical and plasmonic sensors with improved sensitivity. Different types of enzymes have attracted much attention for use in chiral sensing as well. As the structural components of proteins, various peptides and AAs are desirable choices for the construction of chiral sensors utilizing different NMs.[92,93] Herein, we summarize recent development in the combination of proteins, peptides, and AAs with NMs for preparing chiral sensors. The distinctive cooperation approaches are displayed in Table 1. Moreover, the merits of

Table 1 Advantages of combining biomolecules and nanomaterials for chiral sensing

Type of biomolecules	Type of nanomaterials	Applications	Advantages	Ref.
DNA origami	Gold nanorods Gold nanosphere Gold–silver nanorods	Recognizing specific enantiomers investigating chiral photophysical effects and enantioseparation at the nanoscale	Improved response signal High selectivity and sensitivity	53, 55, 58, 60–62 and 64–68
DNA nanoribbon	Gold nanoparticles Gold nanorods	Chiral sensing	Tunable chirality	76
DNA aptamer	Shell core-gold satellites	Detecting ochratoxin A concentrations	Improved detection sensitivity	73
DNA	Carbon nanotubes	Investigating interaction between DNA and chiral carbon nanotubes chiral spintronics	Higher spin polarization degree Enhanced recognition ability	88 and 89
DNA-like structure	Metal–organic frameworks	Recognizing amino acids	Sensitive and rapid detection	87
Bovine serum albumin	Graphene quantum dots	Chiral sensing of tryptophan isomers	Higher chiral discrimination ability	94–99
	Covalent organic frameworks		Enhanced electron transfer efficiency	
	Gold nanorods		Ultrasensitive detection	
Acetylcholinesterase	Graphene	Enantiomeric discrimination of methamidophos	Improved sensitivity	102
D-amino acid oxidase	Fe_3O_4–Au–Ag nanoparticles	Chiral recognizing D-alanine	Enhanced sensitivity	108
Peptide	Gold nanopolyhedrons, gold nanorods, cobalt oxide nanoparticles, nanohelices, nanoribbons, nanosheets, nanofibrils, nanospheres, Cu–Pt nanoparticles	Chiral sensing	Nanoscale controllability of chirality	110–116,119–121
Cysteine	CdTe quantum dots, carbon nanotubes-Polypyrrole-Au nanoparticles, CdS/CdTe NPs	Chiral recognizing amino acids	Enhanced sensitivity	127–130
Histidine	Metal–organic frameworks	Chiral sensing	Improved sensitivity	131
Pyroglutamic acid	CdSe/ZnS quantum dots	Enantiomeric recognition of amino acids	Simplified prepared procedure	132
Lysine	Nanofiber	Enantiomeric discrimination of tryptophan	Desirable enantioselective ability	133
Cyclodextrin	Graphene, nultiwalled carbon nanotubes, black phosphorus nanosheets, copper metal organic framework, titanium dioxide nanotube, gold nanoparticles	Chiral recognizing amino acids	Improved sensing efficiency Satisfactory repeatability and stability	141–146,152–155,161–165
Chitosan	Graphene, carbon nanotube	Chiral recognizing enantiomers	Enhanced sensitivity	171–174
Cellulose	Nanocellulose	Chiral sensing	Desirable stability	175

employing these sensors instead of traditional devices are described in detail.

Owing to multiple binding sites on the selectors surface, proteins possessed satisfactory stereoselective ability. Among various types of proteins, bovine serum albumin (BSA) was extensively investigated selector in chiral sensing. Graphene quantum dots (GQDs)-modified BSA was developed for the chiral sensing of tryptophan (Trp) isomers.[94] Since the amidation reaction between BSA and GQDs could extend the peptide strands of BSA, several cavities were formed within the GQDs-BSA composites (Fig. 3(A)). The combination of GQDs and BSA facilitated the changes in BSA spatial configuration, resulting in the exposure of more chiral sites at the BSA surface. This GQDs-BSA material possessed decreased the hydrophobility and easier accessibility to the target molecules. Furthermore, the GQDs-BSA composites were modified onto the glassy carbon electrode (GCE). The capability of the sensor for recognizing Trp isomers was explored by pulse voltammetry. The results indicated that the oxidation peak currents of the enantiomers could be enhanced at the GQDs/GCE. Nevertheless, the recognition capability of GQDs/GCE was poor due to the few chiral sites on GQDs. Discernible differences in both peak potentials and currents were able to be clearly observed when the BSA/GCE was utilized for the recognition of Trp isomers, indicating that the intrinsic chirality of BSA played an important role in chiral recognition. The proposed sensor presented higher affinity toward L-Trp than D-Trp. Jelinek *et al.* investigated the cooperation of amyloid beta-protein and carbon quantum dots.[95] Amyloid beta-protein played an essential role in forming the fibrillar amyloid plaques in Alzheimer's disease patients' brains. The chiral modulation of amyloid-beta fibrillation and cytotoxicity by enantiomeric carbon quantum dots was explored. Pang *et al.* reported the acceleration of α-synuclein fibril formation and associated cytotoxicity stimulated by silica nanoparticles.[96] We foresee the combination of

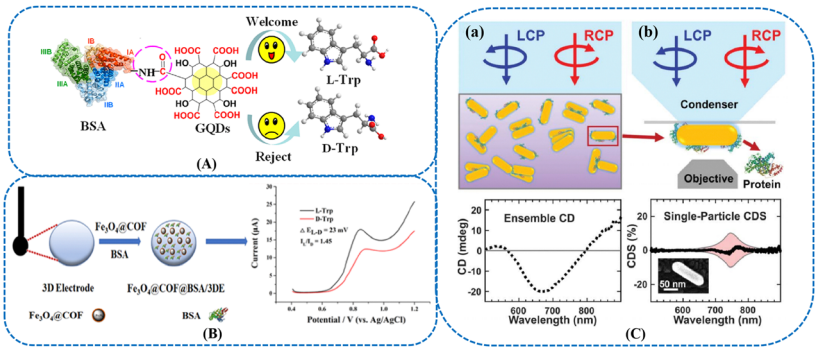

Fig. 3 (A) Covalent functionalization of bovine serum albumin with graphene quantum dots for the chiral recognition of tryptophan isomers.[94] Reprinted from Q. Ye *et al.*, *Anal. Chem.*, 2019, **91**, 11864–11871 Copyright (2019), with permission from American Chemical Society. (B) Synthesis of Fe_3O_4@COF@BSA/3DE, and chiral recognition for Trp enantiomers.[97] Reprinted from L. Wang *et al.*, *Anal. Chem.*, 2021, **93**, 5277–5283 Copyright (2021), with permission from American Chemical Society. (C) (a) Schematic illustration of ensemble CD measurements (top) and PCCD spectrum (bottom) of Au NR–BSA complexes at [BSA] = 1.5 μM. LCP, left-handed circularly polarized light; RCP, right-handed circularly polarized light. (b) Schematic illustration of single-particle CDS measurements (top) and CDS spectrum (bottom) for a single Au NR–BSA complex. The inset shows the correlated scanning electron microscopy (SEM) image.[98] Reprinted from Q. Zhang *et al.*, *Science*, 2019, **365**, 1475–1478 Copyright (2019), with permission from the American Association for the Advancement of Science.

NMs with different types of proteins such as amyloid beta-protein and α-synuclein amyloid fibrils in sensing. The BSA-covalent organic framework (COF) modified 3D-printed electrochemical sensor was constructed for the chiral recognition of Trp (Fig. 3(B)).[97] Compared with a single BSA-based 3D-printed electrode, the introduction of magnetic COF could enhance the electron transfer efficiency. This sensor displayed higher chiral discrimination ability of Trp than the electrode without COF materials. In addition to electrochemical sensor, BSA was used for developing plasmonic sensors as well.[98,99] NR–protein complexes could scatter light with distinct optical polarizations, inducing changes in intensity between right and left circularly polarized light. The chiral GNR–BSA complexes were prepared based on BSA-induced NP aggregation (Fig. 3(C)). During the synthesis process, BSA could transfer chirality to the plasmonic substrates, and the assembly of these complexes was also influenced by BSA.

Plasmon-coupled CD could achieve the ultrasensitive detection of chiral signal by combining surface plasmons and molecular chirality. There were some different chiral sensors, where the signal reading was not according to the CD responses enhancement but CD signal migration.[100,101] Superchiral spectroscopy could detect protein higher order structure at the picogram level depending on the improved sensitivity of superchiral evanescent fields to mesoscale chiral structure. The handedness of chiroptical materials at the nanoscale could be adjusted using macroscale deformations. This macro-to-nano chirality transfer could be extended to various nanoscale components.

As a type of protein, enzymes were also applied for chiral sensing. A graphene chiral sensor with acetylcholinesterase modification was developed for the enantiomeric discrimination of methamidophos.[102] Graphene was considered a desirable candidate for fabricating high-performance sensors due to its satisfactory electrical conductivity, biocompatibility, and ultrahigh surface area.[103–107] The electrical detection of enantiomers could be achieved by transferring the inhibition effect of methamidophos on acetylcholinesterase to graphene. An efficient electrochemical sensor based on Fe_3O_4@Au@Ag@CuxO NPs was fabricated for the chiral recognition of D-AAs.[108] The designed sensor avoided D-AA oxidase (DAAO) immobilization and repeated NMs modification on the electrodes. During the sensing process, DAAO was able to catalyze D-AAs to generate H_2O_2. Also, the presence of H_2O_2 with CuxO shell autocatalytic oxidation reaction could further give rise to a decrease in the electrochemical signals. Fe_3O_4@Au@Ag@CuxO NPs were utilized as electrochemical beacons for the sensitive recognition of D-alanine (D-Ala). To achieve the transmission of chirality from chiral molecules to achiral polymers, the 3D microenvironment-bearing D/L phenylalanine (Phe) chiral centers was designed based on right-handed helical nanostructures.[109] The catalytic capability of lipase immobilized inside the microsystem was obviously enhanced by the proposed microenvironment. In addition, the 3D microenvironment presented desirable storage stability and effective recyclability.

Various chiral nanostructures based on the self-assembled peptides were applied for enantiomeric sensing. The AA sequence in the peptides significantly influences the configuration of chiral nanostructures. Consequently, the nanoscale control of the chirality can be achieved utilizing the programmable sequence of the peptide to direct the chiral NMs growth. Zou *et al.* synthesized gold nanopolyhedrons based on peptide-directed growth, and the resulting peptide (CGGEVSALEK)-modified gold nanopolyhedrons displayed circular dichromatic couplets in the visible region.[110] Results suggested that the chiral optical features of the nanopolyhedrons were affected by their size and spatial structure. The growth of GNPs has been controlled using peptides to create chiral NPs.[111] For instance, chiral GNPs were able to be synthesized by adding peptides or AAs during the NP growth process.[112] The formed chiral composites possessed tunable handedness and chiral plasmonic resonance. Moreover, the peptide sequence of the resulting

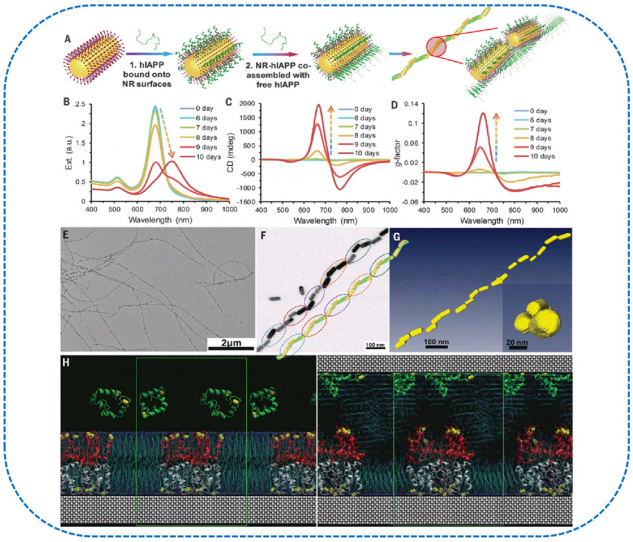

Fig. 4 Assembly of hIAPPs with NRs producing LC-like helices with long-range order. (A) Schematics of the assembly process of hIAPP monomers with NRs. (B) to (D) Extinction (Ext.) (B), CD (C), and g-factor (D) spectra for the coassembly process of 4.0 mM hIAPPs with 0.50 nM gold NRs with average lengths and diameters of 50 and 19 nm, respectively. (E) and (F) TEM images of nanohelices. The nanohelice model in (F) was reconstructed from the TEM images at various tilting angles. The circles represent the pitch of the nanohelices. (G) Reconstructed cryo-TEM tomography images showing the left-handed helices of the straight hIAPP-NR fibers. (H) Initial (left) and final (right) structures for the MD simulations of hIAPPs in the CTAB bilayer. The different hIAPP molecules are depicted as follows: silver ribbons for molecules in the bilayer and in contact with gold, red ribbons for molecules in the bilayer and in contact with the aqueous solution, and green ribbons for the free peptides in solution. The sulfur atoms of hIAPPs are depicted as yellow spheres, the gold atoms as gray spheres, the CTA^+ cations as lines (carbon shown in cyan and nitrogen in dark blue, with hydrogen atoms omitted for clarity), and the Br^- and Cl^- anions as purple dots.[115] Reprinted from J. Lu *et al.*, *Science*, 2021, **371**, 1368–1374 Copyright (2021), with permission from the American Association for the Advancement of Science.

composites could allow dynamic control of the nanostructure chirality.[113] The human islet amyloid polypeptide (hIAPP) possessed the helical structures, and the tape-like structure could be formed based on the β-sheet secondary structure of the peptide.[114,115] Due to the chiral carbon of peptides, this tape-like structure was twisted with a regular pitch. The structural ordering of hIAPP was able to be transferred to the composites by assembling hIAPP with uniform GNRs (Fig. 4). To investigate the synergistic coupling of hIAPP and GNRs, the CD response of the composites was controlled by optimizing the gap distance between the NRs and nanohelix pitch length. The results indicated that improving the long-range order could guide the synthesis of materials with high optical asymmetry. Chiral cobalt oxide NPs were synthesized utilizing L- and D-tyrosine (Tyr)-Tyr-Cysteine (Cys) peptides as ligands.[116] The results suggested that the carboxylic and thiol groups of Tyr-Tyr-Cys displayed strong interaction with the NPs surfaces. During the preparation process, the peptides could transfer the chirality to cobalt oxide NPs and trigger particle formation. Owing to the chirality of Tyr-Tyr-Cys peptides, the resulting hybrid NMs presented mirror-symmetric chiroptic responses. The influence of peptides sequence on preparing chiral NPs was investigated, and the carboxylic group of the peptide played an important role in the NPs chirality expression. Various types of peptides were able to be applied for developing chiral inorganic NMs. In addition, peptides could self-assemble into ordered chiral nanostructures.[117,118] Functional chiral nanostructures were developed by coupling aromatic AAs with meso-tetrakis (4-carboxyphenyl)porphyrin (TCPP).[119] Left-handed nanohelices were able to be obtained *via* the self-assembly of TCPP-Phe4 (TCPP-F4). Moreover, the effect of AAs types on the hierarchical assembly process was explored. For instance, TCPP-L-Trp4 (TCPP-L-W4) facilitated the formation of right-handed nanohelices when Trp replacing the terminal AA Phe. The resulting NMs presented a promising potential in chiral separation and chiral catalysis. The supramolecular nanostructures with different architectures including nanofibrils, nanoribbons, nanohelices, nanosheets, and NSs could be obtained by optimizing the AA sequence of the peptides and the self-assembling condition.[120] The results indicated that the chiral separation efficiency of the peptide nanostructures was affected by their morphology, surface charges, and amino acid sequences of the peptides. Different types of chiral molecules were able to be recognized using various supramolecular nanostructures. Fig. 5(A) shows the molecular structure of Fmoc-Phe-Phe-lysine (Lys) (Fmoc-FFK). Moreover, Fmoc-FFKK and Fmoc-FFKD were respectively prepared by adding a Lys and aspartic acid at the N-terminus of Fmoc-FFK. Under acidic conditions, a right-handed nanohelix could be formed depending on the Fmoc-FFK. The Fmoc-FFKK was able to assemble into nanoribbons, and Fomc-FFKD facilitated the synthesis of nanofibrils and NSs. Glutathione (GSH)-functionalized Cu–Pt NPs were prepared based on the integration of GSH with Cu and Pt NPs *via* Cu–S and Pt–S interactions.[121] This sensor combined the intrinsic chirality of GSH and charge transfer competency of Cu and Pt NPs. Compared with GSH, GSH-modified Cu NPs, and GSH-modified Pt NPs, the resulting GSH-Cu/Pt presented better enantiorecognition ability of Tyr enantiomers. Since three H-bonds were formed between L-Tyr and GSH, GSH-Cu/Pt exhibited higher affinity toward L-Tyr than D-Tyr.

AAs are considered important chiral molecules in nature since they can be applied as biomarkers for diverse metabolic diseases. It is essential to investigate a sensitive and efficient approach for enantiorecognizing AAs enantiomers.[122–126] In addition to Cu-Pt NPs, CdTe QDs were modified with L-Cys for the chiral recognition of Tyr enantiomers.[127] Results also suggested different interactions of L- and D-Tyr with L-Cys/CdTe QDs. The Cys-based QDs possessed a promising potential for chiral and biological sensing.[128] Cys was chosen as the chiral ligand for preparing chiral CdS/CdTe NPs and their rod-shaped superstructures.[129] Moreover, the chiral double helix CNTs (DHCNTs)@Polypyrrole (PPy)@GNPs nanocomposites were prepared for anchoring L/D-Cys.[130] PPy and GNPs were able to synergistically improve the conductivity of this sensor. Since the L/D-Cys and L/D-DHCNTs possessed chiral structure, the

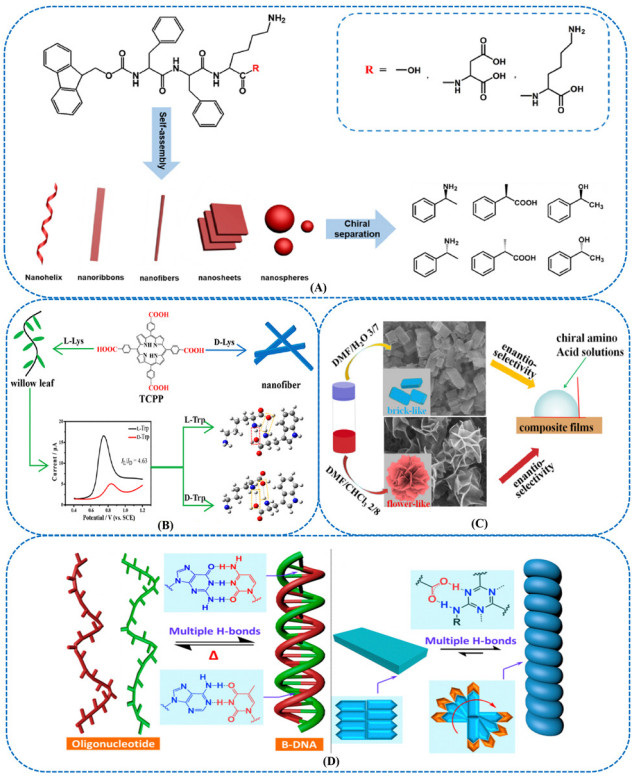

Fig. 5 (A) Schematic diagram of Fmoc-FFK, Fmoc-FFKK, and Fmoc-FFKD assemblies forming supramolecular nanostructures for chiral separation.[120] Reprinted from Y. Fan *et al.*, *Langmuir*, 2020, **36**, 10361–10370 Copyright (2020), with permission from American Chemical Society. (B) Chiral enantioselective assemblies induced from achiral porphyrin by L- and D-Lysine.[133] Reprinted from S. Wu *et al.*, *Langmuir*, 2019, **35**, 16761–16769 Copyright (2019), with permission from American Chemical Society. (C) Chiral flower-like and brick-like nanostructure films *via* solvent-tuned self-assembly and their enantioselective performances toward L-/D-amino acids.[134] Reprinted from K. Chen *et al.*, *Langmuir*, 2019, **35**, 3337–3345 Copyright (2019), with permission from American Chemical Society. (D) Role of multiple hydrogen bonds in the induction and stabilization of a super-chiral B-DNA Structure; utilization of duplex hydrogen bonds among carboxylic acids and various pyridine-based binders to control the emergence of chiral nanostructures.[135] Reprinted from P. Xing *et al.*, *J. Am. Chem. Soc.*, 2019, **141**, 9946–9954 Copyright (2019), with permission from American Chemical Society.

synergy and complementarity effect facilitated the enhancement of sensor sensitivity. This electrochemical sensor exhibited efficient chiral recognition competency toward AA enantiomers such as Tyr, Trp, and glutamic acids (Glu). Hierarchically-structured chiral MOFs were prepared using histidine (His) as the chiral ligand.[131] To achieve the electrodeposition of Zn through the polystyrene bead template, Zn^{2+} was reduced to metallic Zn. Also, macroporous Zn was formed by removing the polystyrene bead template (Fig. 6). Chiral zeolitic imidazolate framework-8 (ZIF-8) was fabricated *via* the interaction between Zn^{2+} produced by Zn electrooxidation and a mixture containing 2-methyl imidazolate and L- or D-His. Compared with flat chiral MOF, this resulting macroporous material presented improved chiral adsorption capability owing to the higher number of adsorption sites. The chiral separation efficiency was able to be

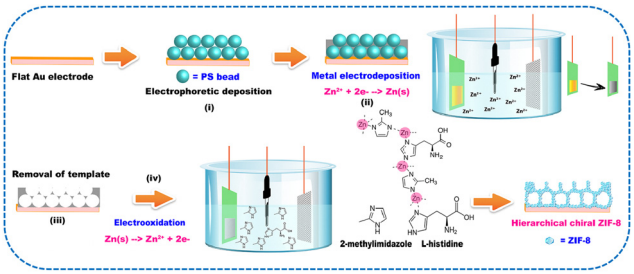

Fig. 6 Illustration of the synthesis steps of hierarchical macroporous chiral ZIF-8, including (i) PS bead assembly *via* electrophoretic deposition, (ii) electrodeposition of macroporous Zn, (iii) removal of PS beads, and (iv) electrodissolution of Zn in the presence of organic ligands.[131] Reprinted from D. Suttipat *et al.*, *ACS Appl. Mater. Interfaces*, 2020, **12**, 36548–36557 Copyright (2020), with permission from American Chemical Society.

optimized using a controllable electric potential to the electrode. In addition, this chiral ZIF-8 material was deposited at the walls of a microfluidic device for enantioseparation. Pyroglutamic acid derivatives were modified with CdSe/ZnS QDs for developing chiral fluorescent nanosensors.[132] Since the sulfhydryl groups of the chiral module facilitated the reaction between CdSe/ZnS QDs and chiral selector, the preparation process could be simplified. The resulting sensor displayed enantiomeric fluorescence response to His, Glu, and dihydroxyphenylalanine. A chiral self-assembly based on achiral porphyrin was developed utilizing L- and D-Lys as the inducers.[133] Compared with L- and D-Lys, the assembly presented expanded configurations due to the introduction of macrocyclic TCPP. Lys played an important role in the chiral recognition process, and the molecular chirality of Lys could be transferred to the assembly. Due to the opposite optical activities of Lys enantiomers, the resulting D-Lys/TCPP and L-Lys/TCPP possessed distinct morphologies. D-Lys/TCPP displayed a nanofiber structure, and L-Lys/TCPP showed a willow leaf-shaped nanostructure (Fig. 5(B)). This chiral self-assembly exhibited desirable enantioselective ability toward Trp isomers. The supramolecular assemblies of AA derivatives and achiral molecules could be achieved under the synergistic effect of intermolecular noncovalent interactions. A variety of hierarchical composite film nanostructures was constructed based on achiral porphyrin derivatives and chiral amphiphilic Glu derivatives.[134] Results indicated that chiral flower- and brick-like nanostructure films were able to be obtained for transferring chirality from the molecular level to complex structures through hydrogen bond (Fig. 5(C)). These self-assembled nanostructures provided an efficient sensor for identifying certain AAs enantiomers. Melamine and its derivatives were satisfactory molecular binders to generate ordered supramolecular structures with aromatic AAs and induce nanoscale chirality. Chiral nanotubes and ribbons could be formed based on the duplex hydrogen bonds formed between the melamine core and serine segments (Fig. 5(D)).[135]

A variety of NMs can be applied for fabricating protein-based chiral sensors. NMs including GQD, COF, and GNR exhibit specific advantages in constructing protein-based electrochemical

and plasmonic sensors. The cooperation between NMs and enzymes such as acetylcholinesterase, DAAO, and lipase provides a simple and efficient approach to realize the sensors' chirality transmission and signal amplification. Due to the programmable sequence of peptides, the proposed sensors are able to control the chirality at the nanoscale. In the investigation of the cooperation between AAs and NMs, the applications of electrochemical and fluorescent nanosensors have attracted much research interest.

2.3. Creating a cooperative relationship between polysaccharides and nanomaterials in chiral sensing

The cooperation of polysaccharides and NMs in chiral sensing has recently attracted tremendous attention due to their exceptional benefits in terms of chiral selectivity, detection sensitivity, operation simplicity, and low cost. Distinct NMs are combined with cyclodextrins (CyDs), chitosan (CS), and cellulose to enhance the electrochemical and colorimetric sensitivity. Since polysaccharides involving multiple chiral centers are considered favorable selectors for NMs modification, the innovative nanocomposites by integrating polysaccharides and NMs have emerged as promising electrochemical sensors. Moreover, polysaccharide-metal NMs are advantageous in colorimetric sensing because of the specific optical properties of GNPs. We now review the novel chiral sensors fabricated *via* the incorporation of polysaccharides and NMs.

As a type of cyclic polysaccharide, β-CyD containing seven glucose units is able to offer a satisfactory chiral microenvironment for generating host–guest inclusion compounds with distinctive chiral molecules. A variety of CyDs and their derivatives have been extensively applied as chiral selectors owing to their wide diversity, nontoxicity, and biodegradable properties.[136–140] Integrating conductive NMs with β-CyD and the sensing film is a desirable strategy to enhance the conductivity of β-CyD, further improving the sensing efficiency. Carbon NMs such as graphene and CNTs have been utilized to modify electrodes for enhancing the detection sensitivity. Yu *et al.* fabricated an electrochemical sensor based on amino-β-CyD (NH_2-β-CyD) and single-layer graphene oxide (SGO) for Tyr enantiomers recognition.[141] A chiral composite was obtained by covalently coupling NH_2-β-CyD with SGO *via* an amidation reaction (Fig. 7). The proposed nanocomposite was assembled with black phosphorus nanosheets (BPNSs) for further modifying a GCE. This fabricated sensor could be employed for the selective recognition of Tyr enantiomers. The applicability of the resulting sensor for chiral recognizing Tyr enantiomers was investigated by square wave voltammetry. The sensor exhibited a relatively higher affinity for D-Tyr with a lower oxidation peak potential and a higher oxidation peak current. Based on a signal-to-noise ratio of 3 (S/N = 3), the limits of detection values of D-Tyr and L-Tyr at SGO-NH_2-β-CyD/BPNSs/GCE were 1.02 and 1.74 μM, respectively. There was a desirable relationship between the Tyr concentrations and the peak currents. Consequently, Tyr enantiomers were able to be efficiently quantified. The results indicated that covalent coupling and self-assembly methodologies were beneficial for improving the detection sensitivity. Depending on the chiral properties of

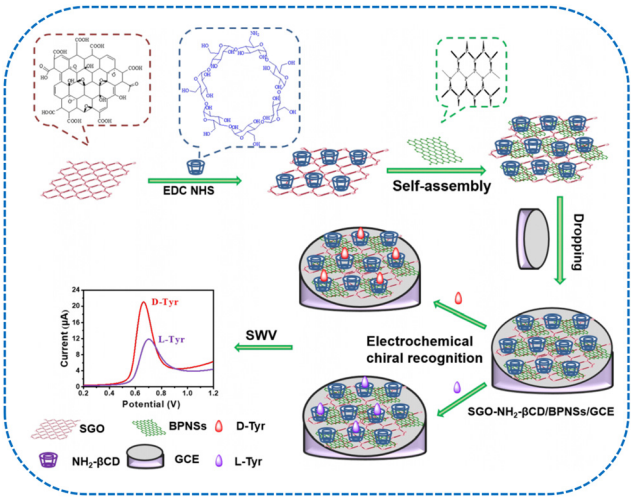

Fig. 7 Preparation of a chiral sensor SGO-NH_2-βCD/BPNSs/GCE for the electrochemical recognition of Tyr enantiomers.[141] Reprinted from J. Zou *et al., ACS Appl. Nano Mater.*, 2021, **4**, 13329–13338 Copyright (2021), with permission from American Chemical Society.

NH_2-β-CyD and electrochemical behaviors of 3,4,9,10-perylene tetracarboxylic acid-modified graphene (rGO-PTCA), an efficient chiral sensor was developed employing a CyD-functionalized graphene for recognizing Phe enantiomers.[142] The resulting rGO-PTCA-CyD exhibited better recognition ability than the individual NH_2-β-CyD and rGO-PTCA. This composite possessed satisfactory repeatability and stability. Mo *et al.* developed GO-ferrocene (Fc) composites based on the π–π interaction.[143] The obtained GO-Fc composites possessed large surface area and high loading. A one-pot strategy was further applied for introducing β-CyD on GO-Fc. After coating the corresponding β-CyD-GO-Fc onto a GCE, an electrochemical sensing platform was fabricated for recognizing Phe enantiomers. The development of materials with electroactive units usually involves complicated reaction steps. It is necessary to explore simple processes for preparing the materials. A chiral selector was developed based on Cu(II) ions-coordinated β-CyD self-assembly on carboxymethyl cellulose (CMC).[144,145] The combination of N-doped reduced GO (N-rGO) and CyD-Cu-CMC facilitated the recognition of Trp enantiomers with a stronger electrochemical signal for L-Trp. To induce the chiral signal, it is necessary to integrate the achiral molecule with another chiral material. The encapsulation of achiral chromophore guest within the chiral cavity of CyD facilitates the generation of an induced CD.[146] The transformation between supramolecular chirality and assembly conformational transition has attracted tremendous attention in exploring the chirality phenomenon in life and nature.

Due to their large surface area and desirable electrochemical property, multiwalled CNTs (MWCNTs) are considered favorable materials for fabricating electrochemical sensors.[147–151] To avoid the agglomeration effect of MWCNTs, functionalized CNTs have attracted widespread interest. An electrochemical sensor based on β-CyD and Fc-functionalized MWCNTs was fabricated for sensing Trp isomers with a desirable enantioselectivity coefficient of 5.78.[152] A chiral sensor was

developed by modifying the GCE with hydroxypropyl β-CyD crosslinked MWCNT.[153] Drugs possessing multiple chiral centers present a greater threat to human health owing to more number of enantiomers as compared to that of a single enantiomeric drug. The resulting electrochemical sensor was applied for discriminating atorvastatin isomers. MWCNTs were regarded suitable NMs for developing chiral interfaces due to their high surface area, desirable biocompatibility, and conductivity. A chiral sensor was designed *via* the self-assembly of Cu^{2+}-functionalized β-CyD on poly-L-arginine/MWCNTs for sensing Trp enantiomers.[154] A good linear correlation in the range of 1×10^{-6} M–5.5×10^{-5} M was obtained. A multilayer nanocomposite consisting of amino-functionalized β-CyD (NH_2-β-CyD), gold–platinum core–shell microspheres (Au@Pts), and MWCNTs was modified onto a GCE.[155] This electrochemical sensor presented satisfactory enantiorecognition ability and repeatability for separating the Trp enantiomers.

Among diverse analytical technologies used for recognizing chiral molecules, electrochemical sensors present specific advantages such as simple operation, high sensitivity, and low cost.[156–160] In addition to carbon NMs, other types of NMs can provide desirable platforms for sensing as well. To discriminate ethambutol (ETB) isomers, an enantioselective electrochemical sensor was developed utilizing a β-CyD-based copper MOF (CyD-CuMOF) as a chiral host.[161] This CyD-CuMOF and carbon nanofibers (CNF) composite material was modified onto a GCE. Also, the proposed working electrode was able to provide chiral environment for ETB isomer recognition depending on the difference in complexation ability using voltammetry. As a type of phosphorene, black phosphorus (BP) is highly similar to graphite. Nafionstabilized BPNSs and 6-O-α-maltosyl-β-CyD (G2-β-CyD) composite were fabricated for the recognition of Trp enantiomers.[162] The proposed platform exhibited satisfactory stability and desirable reproducibility as well as anti-interference ability. In addition, Yu *et al.* also utilized BPNSs and G2-β-CyD-functionalized GCE for the discrimination of Tyr enantiomers.[163] The results indicated that Tyr isomers and G2-β-CyD/BPNSs could selectively generate intermolecular hydrogen bonds for chiral recognition. Nowadays, artificial solid-state nanochannels possessing ionic current rectification ability have displayed promising chiral discrimination activity for AAs. Titanium dioxide (TiO_2) nanochannel arrays formed with TiO_2 nanotubes were constructed for chiral sensing using amino-substituted β-CyD as the chiral recognition elements.[164] This nanochannel-based sensor was able to efficiently discriminate His enantiomers. Moreover, the high-throughput detection of multiple chiral molecules could be achieved by introducing distinctive chiral recognition units. Gold NMs have been extensively used in the analysis domain owing to their prominent optical characteristics. Since bare GNPs are easy to aggregate because of their high surface energy, it is necessary to protect the GNPs surface utilizing capping molecules for developing a steric barrier between the dispersed NPs. Macrocyclic supramolecules such as α-, β-, and γ-CyDs possessing satisfactory cavity size and simple availability are considered favorable candidates for GNPs surface modification. The innovative hybrid NMs prepared by integrating GNPs and supramolecular macrocycles have emerged as promising nanosensors. Compared with native CyDs, anionic CyDs derivatives exhibit specific advantages for chiral sensing. Sugammadex (SUG) is a type of carboxylic acid-modified γ-CyD derivative. The SUG-protected GNPs were prepared *via* a one-pot approach without using additional reducing reagents.[165] This supramolecular-metal hybrid NM could be applied as an efficient colorimetric sensor based on the combination of SUG chiral structure and GNPs optical characteristics.

Natural polysaccharides including CS and soluble starch (SS) possessed desirable enantiorecognition ability due to multiple chiral identification sites.[166–170] In addition to β-CyD, CS was modified with rGO-PTCA *via* the amidation reaction as well. The GCE functionalized with rGO-PTCA-CS was utilized for sensing Trp enantiomers.[171] Since rGO-PTCA-CS composites displayed higher enantiorecognition potency to L-Trp than D-Trp, a higher electrochemical signal was observed at the GCE in L-Trp. A novel polysaccharide chiral selector (SA-CS) was developed *via* an amidation reaction between sodium alginate and CS (Fig. 8(A)).[172] Furthermore, three-dimensional

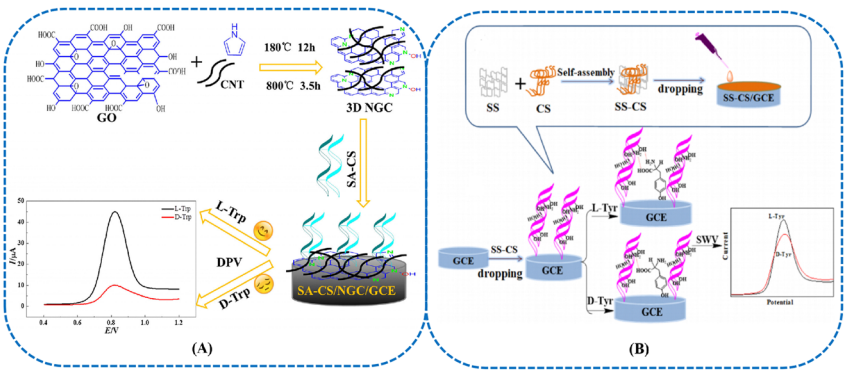

Fig. 8 (A) Diagram of the construction of the SA-CS-NGC/GCE chiral sensing platform.[172] Reprinted from X. Niu *et al.*, *Bioelectrochemistry*, 2020, **131**, 1–11 Copyright (2020), with permission from Elsevier. (B) The preparation of SS-CS/GCE and the proposed mechanism for the chiral electrochemical recognition of Tyr enantiomers on SS-CS/GCE.[173] Reprinted from J. Zou *et al.*, *Talanta*, 2019, **195**, 628–637 Copyright (2019), with permission from Elsevier.

N-doped graphene-CNT (NGC) was combined with SA-CS for the electrochemical measurements of Trp enantiomers. An electrochemical sensor based on the synergistic effect of CS-SS composite-functionalized GCE displayed enhanced capability for recognizing Tyr enantiomers (Fig. 8(B)).[173] The resulting electrochemical sensor was applied for the chiral recognition of D-Tyr and L-Tyr by square wave voltammetry. Based on a signal-to-noise ratio of 3 (S/N = 3), the detection limits of SS-CS/GCE for D-Tyr and L-Tyr were calculated to be 0.42 μM and 0.35 μM, respectively. These results suggested that the chiral sensor displayed satisfactory detection capability for Tyr enantiomers. Complexes containing CS and CS succinamide with CyDs were chosen as chiral selectors for fabricating voltammetric sensors.[174] This system presented desirable enantioselective recognition ability toward atenolol (ATN) enantiomers. Hierarchical nanocellulose (hNC) nanostructures were assembled from long flexible nanofibers and short, rigid nanocrystals.[175] The resulting co-assembled biomaterials presented a uniform chiral nematic-like organization with brilliant iridescent appearance and increased toughness. Compared with conventional chiral cellulose films, this chiral nanocellulose was much tougher.

Polysaccharides provide a promising alternative for developing chiral sensors. Different NM-polysaccharides cooperation strategies have been discussed in this section, and the referenced work indicate that polysaccharide-based nanosensors present specific merits in chiral sensing.

3. A cooperation tale of biomolecules and nanomaterials in chiral separation

The cooperation of biomolecules and NMs can provide a satisfactory platform for chiral sensing. Novel cooperation approaches have been mainly focused on realizing chiral transfer, signal amplification, and sensitivity enhancement. Biomolecules-based chiral nanosensors have attracted tremendous attention nowadays. It can be an inspiration to the cooperation of biomolecules and NMs in microscale chiral separation. These NMs possess large surface area, enabling the improvement of biomolecules immobilization efficiency and chiral separation performance. Herein, we review the distinct NMs used to fabricate biomolecules-based microscale chiral separation systems (Table 2).

3.1. Creating a cooperative relationship between proteins and nanomaterials in chiral separation

Proteins can be employed to develop novel chiral sensors *via* NMs-based approaches. The advantages of cooperating proteins and NMs for chirality amplification are highlighted in Section 2.2. For developing microscale chiral separation systems, NMs immobilization provides a desirable strategy to introduce proteins into capillary columns. Distinct NMs have been introduced into open tubular (OT) and monolithic capillaries to construct BSA or enzymes-based chiral separation microenvironments.

Owing to their various binding sites on the surface, the protein-based chiral stationary phase presents desirable enantioselectivity for different types of enantiomers.[176–178] To investigate the influence of carboxylated MWCNTs on the electrophoretic enantioseparation performance, a chiral stationary phase based on BSA-conjugated MWCNTs was developed for separating ketoprofen, ibuprofen, uniconazole, and hesperidin enantiomers.[179] During the preparation process, BSA/MWCNTs conjugates were immobilized onto the (3-aminopropyl)triethoxysilane (APTES)-functionalized OT capillary. The results indicated that MWCNTs with carboxylic functional groups could improve the BSA immobilization efficiency and enhance the enantioseparation performance. The resulting columns exhibited desirable repeatability and with the batch-to-batch, day-to-day, and run-to-run relative standard deviations (RSDs) of migration times less than 3.5%. An innovative OT chiral column was developed based on BSA and ZIF-8 (Fig. 9).[180] The developed nanocomposites presented specific advantages for enantioseparation by combining the high surface areas of ZIF-8 and diverse chiral binding sites of BSA. Depending on the synergistic effect of ZIF-8 and BSA, nine groups of molecules including homologues, isomers, and enantiomers were successfully baseline separated. The obtained column exhibited desirable separation stability in terms of run-to-run, day-to-day, column-to-column, and batch-to-batch reproducibility. The proteinaceous phase-transitioned BSA (PTB) film was modified onto the capillary inner wall for enantioseparation.[181] Compared with being utilized as a chiral additive in running buffer, BSA used as the stationary phase presented enhanced chiral separation ability, and the adsorption problem could be avoided. These PTB film-coated capillary columns exhibited satisfactory repeatability in terms of the separation efficiency and migration time.

Table 2 Advantages of biomolecules-based microscale chiral separation systems

Type of biomolecules	Type of nanomaterials	Applications	Advantages	Ref.
Bovine serum albumin	Multiwalled carbon nanotubes Zeolite imidazolate framework-8	Chiral separation of chiral drugs	Improve the immobilization efficiency, Enhanced enantioseparation performance, Desirable repeatability and stability	179 and 180
Pepsin	Zeolite imidazolate framework-8, Gold nanoparticles	Enantioseparation of chiral drugs	Higher enantioseparation capability, Improved stability	182–184
Cyclodextrin	Gold nanoparticles, SiO_2 nanoparticles, Magnetic nanoparticles, poly(glycidyl methacrylate)nanoparticles, metal organic framework, quantum dots	Enantioseparation of amino acids, chiral drugs	Improved enantioseparation performance Satisfactory repeatability	192, 195–198 and 202–207

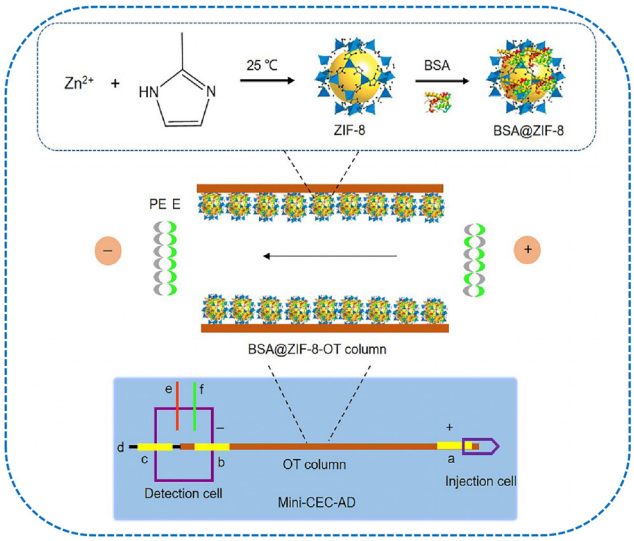

Fig. 9 The schematic diagram of mini-CEC-AD system with BSA@ZIF-8-OT chiral column. (a) Tube electrode for applying high-voltage; (b) and (c) tube electrodes for grounding; (d) working electrode; (e) auxiliary electrode; and (f) reference electrode.[180] Reprinted from T. Wang *et al.*, *J Chromatogr. A*, 2020, **1625**, 1–7 Copyright (2020), with permission from Elsevier.

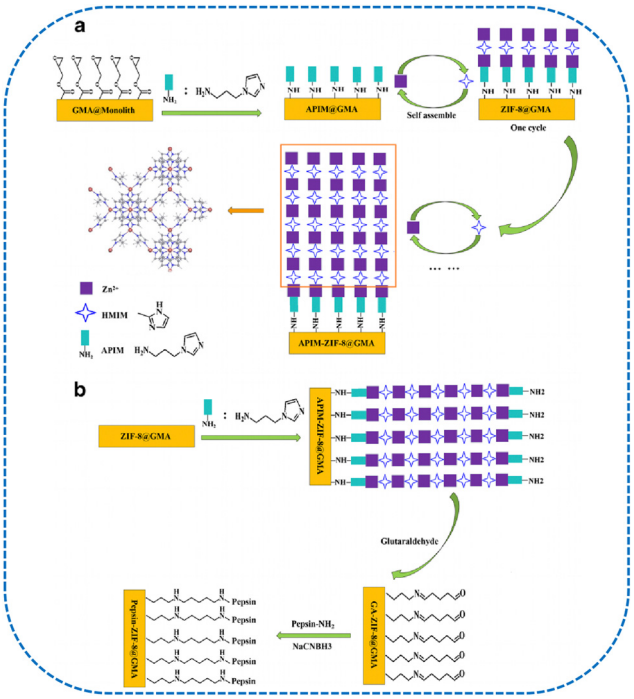

Fig. 10 (a) Scheme for the preparation of ZIF-8@GMA monolithic column and (b) Pepsin-ZIF-8@GMA monolithic column.[182] Reprinted from W. Ding *et al.*, *Microchimica Acta*, 2020, **187**, 1–10 Copyright (2020), with permission from Springer Nature.

ZIF-8 was grown onto the surface of poly(glycidyl methacrylate)-*co*-(ethylene dimethacrylate) [poly(GMA-*co*-EDMA)] monoliths based on layer-by-layer self-assembly (Fig. 10).[182] Furthermore, pepsin chiral selector was covalently immobilized with the amino-modified ZIF-8 *via* the Schiff base approach. The resulting columns presented desirable enantioseparation ability for six enantiomers including amlodipine, hydroxyzine, hydroxychloroquine, chloroquine, nefopam, and clenbuterol. Due to the employment of ZIF-8, higher enantioseparation capability was obtained when compared with a pepsin-functionalized monolithic column without ZIF-8 NPs. GNPs were introduced to poly(GMA-*co*-EDMA) monoliths *via* the Au–S bond.[183] Furthermore, chiral selector pepsin was attached to GNPs based on the hydrochloride/*N*-hydroxysuccinimide coupling reaction. The obtained chiral column exhibited improved enantioselectivity toward chiral drugs such as amlodipine, hydroxyzine, labetalol, hydroxychloroquine, chloroquine, nefopam, clenbuterol, and chlorpheniramine. The results indicated that the GNPs size could influence the column enantioresolution efficiency. Novel material ZIF-4, 5-imidazoledicarboxylic acid (ZIF-IMD), was layer-by-layer assembled onto the pore surface of the porous layer OT (PLOT) capillary column.[184] Chiral selector pepsin was introduced into the column utilizing ZIF-IMD hybrids as solid-phase carriers. The employment of the ZIF-IMD material could improve the stability and chiral separation ability of the PLOT column. Lysozyme supramolecular membrane could be utilized as the chiral selector for CEC chiral resolution.[185] *Candida antarctica* lipase B was successfully immobilized onto the capillary inner wall for the enantioseparation of monoamine neurotransmitter enantiomers including phenylephrine, norepinephrine, and epinephrine.[186]

3.2. Creating a cooperative relationship between polysaccharides and nanomaterials in chiral separation

NMs are considered satisfactory carriers for proteins immobilization owing to their high surface area.[187–191] In addition to proteins, polysaccharides can also be introduced into capillary columns utilizing a variety of NMs including GNPs, SiO_2NPs, magnetic NPs (MNPs), poly(glycidyl methacrylate) (PGMA) NPs, MOFs, and QDs. The effects of NMs on β-CyD and γ-CyD immobilization are discussed in detail. The cooperation of polysaccharides and NMs in capillary microscale systems has been widely applied in chiral separation.

The GNPs-based capillary was applied for modifying polydopamine/sulfated-β-CyD (PDA/S-β-CyD).[192] Owing to their specific stability and high surface-to-volume ratio, GNPs have attracted tremendous attention in CEC separation.[193,194] The phase ratio and surface area of the capillary could be enhanced after introducing GNPs, further improving the enantioseparation performance. The resulting column exhibited increased chiral separation ability compared with the PDA/S-β-CyD-based column without GNPs. The satisfactory stability of PDA/S-β-CyD-GNPs-coated capillary for enantioseparation was obtained as well. A composite NM GNPs-graphitic carbon nitride (GNPs-*g*-C_3N_4) was modified with sulfydryl-β-CyD (HS-β-CyD) for developing CEC chiral stationary phase.[195] GNPs were considered desirable NMs for improving the surface area and changing the surface chemistry of supporting materials. In addition, as a two-dimensional lamellar structure material, g-C_3N_4 nanosheets possessed desirable thermal and chemical stability.

The resulting column exhibited improved separation performance compared with the CyD-GNPs column and CyD-*g*-C_3N_4 column. Satisfactory repeatability was obtained by calculating the RSDs of run-to-run, batch-to-batch, and day-to-day. A β-CyD-GNPs-coated column was prepared *via* the sol–gel approach.[196] The column exhibited favorable enantioseparation capability after being modified with GNPs. A 3-mercaptopropyl-trimethoxysilane (MPTMS)-functionalized capillary column was developed for the layer-by-layer self-assembly of GNPs.[197,198] Then, the self-assembly–fabricated multilayer GNPs column was further utilized to modify with thiols β-CyD (SH-β-CyD). The preparation procedure could be optimized to increase the loading capacity of the chiral selector. Though OT capillary electrochromatography (OTCEC) microsystems possess the ease of fabrication and operation process compared with traditional-packed capillary columns, OT capillary suffered from the relatively low phase ratio and sample capacity. The GNPs were considered a desirable electrochromotographic support to improve the phase ratio of the OTCEC column and then enhance the chiral separation ability in CEC. Depending on their large surface-to-volume ratio, NP-functionalized OT capillary presented promising potential to improve the separation efficiencies of complex samples.[199–201]

To develop chiral OTCEC, zeolite SiO_2NPs were modified with β-CyD or β-CyD/L-Phe.[202] Owing to their high surface-to-volume ratio and easy modification property, NPs could be used as a stationary phase to enhance the separation efficiency. Moreover, CyDs with hydrophobic cavity and hydrophilic edge were able to form host–guest inclusions with the analytes and achieve chiral separation depending on the difference in the effective mobility of the diastereoisomeric complexes. The resulting column exhibited desirable enantioseparation ability toward four chiral analytes including atechin/epicatechin, ephedrine/pseudoephedrine, ritodrine, and salbutamol. MNPs coated with β-CyD and mono-6-deoxy-6-(1-methylimidazolium)-β-CyD tosylate were prepared for developing chiral capillary columns.[203] During the preparation process, the external magnetic field was utilized to immobilize the MNPs onto the capillary inner wall. This preparation approach based on the magnet was quite simple compared with the conventional strategy. The resulting microsystem could be used for enantioseparating dansylated AAs with improved resolution. The capillary based on ethanediamine (EDA)-β-CyD and PGMA NPs was developed for enantioseparation.[204] First, the inner wall of a capillary was modified with glycidyl methacrylate (GMA) to form tentacle-type coating, and then the PGMA NPs were functionalized with the GMA coating. Finally, the chiral selector EDA-β-CyD was covalently immobilized onto the PGMA NPs. The results indicated that PGMA NPs were desirable coating materials for improving the column chiral separation performance. The metal organic framework (MOF) HKUST-1–based CEC enantioseparation system was constructed by choosing carboxymethyl-β-CyD (CM-β-CyD) as the chiral selector.[205] Compared with fused capillary column, the HKUST-1–functionalized column presented enhanced separation performance for five basic drugs including propranolol, esmolol, metoprolol, amlodipine, and sotalol. As a type of porous NMs, MOFs composing metals and organic linkers were applied for developing γ-CyD-MOFs chiral stationary phase in CEC separation.[206] The resulting column could be utilized to separate five chiral Dns-AAs with desirable stability and repeatability. Three types of composite QDs were synthesized by combining the fluorescent property of QDs with the chiral recognition capacity of β-CyD and its derivatives (2-hydroxypropyl-β-CyD, HP-β-CyD; sulfobutyl-β-CyD, SBE-β-CyD).[207] The obtained composite QDs were added into the running buffer as the pseudo-stationary phase. Six groups of model enantiomers could be separated without involving complicated capillary column preparation and analyte derivatization processes.

3. Conclusion

The cooperative relationship between biomolecules and NMs constitutes a wonderful tale about nanoscale chiral sensing and separation. Biomolecules such as DNA, proteins, and polysaccharides exhibit intrinsic chiral recognition capability toward multifarious enantiomers. Meanwhile, NMs possess specific physicochemical properties and have gained wide popularity in amplifying the biomolecules' chirality and improving the assay performance. We reviewed the cooperation strategies of biomolecules and NMs for fabricating chiral sensors and separation systems (Fig. 11).

For the development of DNA-based chiral sensors, studies have mainly focused on synthesizing metal NMs chiral plasmonic systems. A remarkable effort has been devoted to designing pure DNA nanostructures, including DNA origami and nanoribbons. This cooperative relationship between DNA and NMs displays substantial advantages in constructing tailoring sensors with nanometer precision. Since metal NMs present specific plasmonic characteristics, the cooperation of DNA nanostructures and metal NMs can realize chirality transmission and sensitivity enhancement. The influences of NMs on the performance of chiral nanosensors have been described in detail. We found that the state-of-the-art DNA-based chiral sensors containing multiple chiral centers are able to show significant merits for the simultaneous sensing of multiple

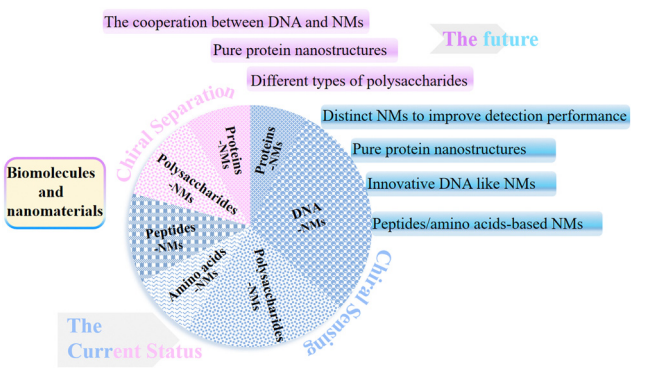

Fig. 11 The current status and future prospects of the cooperation between biomolecules and nanomaterials in nanoscale chiral sensing and separation.

targets. Moreover, the gold–silver NRs discussed in this manuscript indicate that the cooperation concept reveals a promising potential for fabricating bimetallic particles-involved chiral sensors with improved sensitivity. Further researches must exploit the combination of distinct NMs to improve the detection performance. To prepare DNA-like NMs, a novel cooperative relationship between DNA and HMOF-1 has been created. We believe that more work should be focused on exploring innovative DNA-like NMs for chiral sensing. In addition to metal NMs, CNT is a favorable candidate to develop DNA-based sensors with enhanced detection performance. Since enantiomers exhibit different biological and pharmacological activities, developing rapid and sensitive chiral sensing and separation strategies has attracted tremendous attention nowadays. The combination of DNA and NMs presents a prospective trend in developing chiral sensors. In addition, more attention can be paid toward integrating RNA and NMs for chiral sensing. The CE technique facilitates the transformation of a chiral recognition event into identifiable electrochromatographic signals. The marriage of CE and enantiorecognition offers a favorable channel for chiral separation. Nevertheless, the application of DNA/RNA for CE chiral separation is seldom reported. We foresee a growing interest in the cooperation between DNA/RNA and NMs in nanoscale chiral separation.

The variety of protein–NM complexes summarized in this review indicate that the cooperation between NMs and proteins is suitable for enhancing the performance of chiral sensing and separation. New chiral electrochemical and plasmonic sensors have been described in detail, and the substantial merits of NMs in sensors construction are included in the discussion. BSA and enzymes are desirable chirality donors for enantiorecognizing specific analytes. Studies suggest that NM–proteins cooperation enables chirality transmission and signal amplification. Considering the noteworthy benefits of protein–NM complexes, we believe that much more attention should be paid to developing different types of pure protein nanostructures-based chiral sensors and separation systems. In addition, peptides with programmable sequences possess tremendous potential for controlling the sensors chirality at the nanoscale. To explore efficient chiral sensors, NMs have been cooperated with multifarious peptides or AAs. Further work can seek new NMs for the construction of peptides/AAs-based capillaries and discuss the influences of NMs on chiral separation.

Diverse strategies have been applied to develop polysaccharides-based chiral sensors and separation systems. The cooperation of NMs and polysaccharides provides a valuable way to improve the electrochemical and colorimetric sensitivity. We mainly introduce the merits of using CyD-functionalized carbon NMs for chiral sensing. Moreover, metal NMs are employed to construct CyD-based sensors as well. The effects of NMs on CS- and cellulose-based sensors performance have been described in detail. Due to their high surface area, NMs are regarded as favorable carriers for polysaccharide immobilization. The enormous advantages of NMs in introducing polysaccharides into capillaries are included in the manuscript. The most used chiral separation column was based on the coupling of NMs and saccharide or cellulose derivatives. We believe that different types of polysaccharides need to be further explored to broaden the application of polysaccharides-based systems for chiral separation.

This paper narrates the cooperation between biomolecules and NMs in nanoscale chiral sensing and separation. We hope the perpetual relation will continue to compose intriguing chapters for nanoscale chirality.

Author contributions

Tingting Hong and Zhiqiang Cai were involved in project conceptualization, supervision, investigation, writing – original draft, writing – review and editing, as well as funding acquisition. Wenhu Zhou and Songwen Tan were involved in resources and writing – original draft.

Conflicts of interest

There are no conflicts to declare.

Acknowledgements

For financial support of this work, we acknowledge the National Natural Science Foundation of China (81803495).

References

1 J. A. Cowan and R. J. Furnstahl, Origin of chirality in the molecules of life, *ACS Earth Space Chem.*, 2022, **6**, 2575–2581.
2 D. Sanz-Hernández, A. Hierro-Rodriguez, C. Donnelly, J. Pablo-Navarro, A. Sorrentino, E. Pereiro, C. Magén, S. McVitie, J. María de Teresa, S. Ferrer, P. Fischer and A. Fernández-Pacheco, Artificial double-helix for geometrical control of magnetic chirality, *ACS Nano*, 2020, **14**, 8084–8092.
3 A. Horrer, Y. Zhang, D. Gérard, J. Béal, M. Kociak, J. Plain and R. Bachelot, Local optical chirality induced by near-field mode interference in achiral plasmonic metamolecules, *Nano Lett.*, 2020, **20**, 509–516.
4 B. H. Lee, N. A. Kotov and G. Arya, Reconfigurable chirality of DNA-bridged nanorod dimers, *ACS Nano*, 2021, **15**, 13547–13558.
5 Z. Xu, W. Duan and Y. Xu, Controllable chirality and band gap of quantum anomalous hall insulators, *Nano Lett.*, 2023, **23**, 305–311.
6 S. Xie, L. Ai, C. Cui, T. Fu, X. Cheng, F. Qu and W. Tan, Functional aptamer-embedded nanomaterials for diagnostics and therapeutics, *ACS Appl. Mater. Interfaces*, 2021, **13**, 9542–9560.
7 X. Y. Wong, A. Sena-Torralba, R. Álvarez-Diduk, K. Muthoosamy and A. Merkoçi, Nanomaterials for nanotheranostics: tuning their properties according to disease needs, *ACS Nano*, 2020, **14**, 2585–2627.

8 X. Wang, X. Zhong, J. Li, Z. Liu and L. Cheng, Inorganic nanomaterials with rapid clearance for biomedical applications, *Chem. Soc. Rev.*, 2021, **50**, 8669–8742.
9 H. Zhang, S. Li, A. Qu, C. Hao, M. Sun, L. Xu, C. Xu and H. Kuang, Engineering of chiral nanomaterials for biomimetic catalysis, *Chem. Sci.*, 2020, **11**, 12937–12954.
10 M. Sun, X. Wang, X. Guo, L. Xu, H. Kuang and C. Xu, Chirality at nanoscale for bioscience, *Chem. Sci.*, 2022, **13**, 3069–3081.
11 Z. Pei, H. Lei and L. Cheng, Bioactive inorganic nanomaterials for cancer theranostics, *Chem. Soc. Rev.*, 2023, **52**, 2031–2081.
12 Z. Wang, P. Li, L. Cui, J. Qiu, B. Jiang and C. Zhang, Integration of nanomaterials with nucleic acid amplification approaches for biosensing, *Trends Anal. Chem.*, 2020, **129**, 115959.
13 C. Lu, S. Zhou, F. Gao, J. Lin, J. Liu and J. Zheng, DNA-mediated growth of noble metal nanomaterials for biosensing applications, *Trends Anal. Chem.*, 2022, **148**, 116533.
14 S. Bera, B. Xue, P. Rehak, G. Jacoby, W. Ji, L. J. W. Shimon, R. Beck, P. Kral, Y. Cao and E. Gazit, Self-assembly of aromatic amino acid enantiomers into supramolecular materials of high rigidity, *ACS Nano*, 2020, **14**, 1694–1706.
15 J. Yang, M. Chen, H. Lee, Z. Xu, Z. Zhou, S. Feng and J. T. Kim, Three-dimensional printing of self-assembled dipeptides, *ACS Appl. Mater. Interfaces*, 2021, **13**, 20573–20580.
16 C. Liang, Z. Wang, T. Xu, Y. Chen, D. Zheng, L. Zhang, W. Zhang, Z. Yang, Y. Shi and J. Gao, Preorganization increases the self-assembling ability and antitumor efficacy of peptide nanomedicine, *ACS Appl. Mater. Interfaces*, 2020, **12**, 22492–22498.
17 Y. Chen, W. Sun, C. Yang and Z. Zhu, Scaling up DNA self-assembly, *ACS Appl. Bio Mater.*, 2020, **3**, 2805–2815.
18 J. Zhan, Y. Cai, S. Ji, S. He, Y. Cao, D. Ding, L. Wang and Z. Yang, Spatiotemporal control of supramolecular self-assembly and function, *ACS Appl. Mater. Interfaces*, 2017, **9**, 10012–10018.
19 A. Ebrahimi, H. Ravan and S. Khajouei, DNA nanotechnology and bioassay development, *Trends Anal. Chem.*, 2019, **114**, 126–142.
20 J. Huang, W. Ma, H. Sun, H. Wang, X. He, H. Cheng, M. Huang, Y. Lei and K. Wang, Self-assembled DNA nanostructures-based nanocarriers enabled functional nucleic acids delivery, *ACS Appl. Bio Mater.*, 2020, **3**, 2779–2795.
21 N. Xie, H. Wang, K. Quan, F. Feng, J. Huang and K. Wang, Self-assembled DNA-based geometric polyhedrons: construction and applications, *Trends Anal. Chem.*, 2020, **126**, 115844.
22 J. Sun and X. Sun, Recent advances in the construction of DNA nanostructure with signal amplification and ratiometric response for miRNA sensing and imaging, *Trends Anal. Chem.*, 2020, **127**, 115900.
23 W. Wang, S. Yu, S. Huang, S. Bi, H. Han, J. Zhang, Y. Lu and J. Zhu, Bioapplications of DNA nanotechnology at the solid-liquid interface, *Chem. Soc. Rev.*, 2019, **48**, 4892–4920.
24 Y. Peng, H. Pang, Z. Gao, D. Li, X. Lai, D. Chen, R. Zhang, X. Zhao, X. Chen, H. Pei, J. Tu, B. Qiao and Q. Wu, Kinetics-accelerated one-step detection of MicroRNA through spatially localized reactions based on DNA tile self-assembly, *Biosens. Bioelectron.*, 2023, **222**, 114932.
25 E. Benson, R. C. Marzo, J. Bath and A. J. Turberfield, A DNA molecular printer capable of programmable positioning and patterning in two dimensions, *Sci. Rob.*, 2022, **7**, 1–8.
26 A. R. Thomas, K. Swetha, C. K. Aparna, R. Ashraf, J. Kumar, S. Kumar and S. S. Mandal, Protein fibril assisted chiral assembly of gold nanorods, *J. Mater. Chem. B*, 2022, **10**, 6360–6371.
27 H. Wang, Y. Liu, J. Yu, Y. Luo, L. Wang, T. Yang, B. Raktani and H. Lee, Selectively regulating the chiral morphology of amino acid assisted chiral gold nanoparticles with circularly polarized light, *ACS Appl. Mater. Interfaces*, 2022, **14**, 3559–3567.
28 B. L. Li, J. J. Luo, H. L. Zou, Q. M. Zhang, L. B. Zhao, H. Qian, H. Q. Luo, D. T. Leong and N. B. Li, Chiral nanocrystals grown from MoS_2 nanosheets enable photothermally modulated enantioselective release of antimicrobial drugs, *Nat. Commun.*, 2022, **13**, 1–13.
29 Y. Qiu, S. Cao, C. Sun, Q. Jiang, C. Xie, H. Wang, Y. Liao and X. Xie, Thermotropic chirality enhancement of nanoparticles constructed from foldamer/bis(amino acid) complexes, *Polym. Chem.*, 2022, **13**, 4569–4577.
30 S. Vecchioni, B. Lu, J. Janowski, K. Woloszyn, N. Jonoska, N. C. Seeman, C. Mao, Y. P. Ohayon and R. Sha, The rule of thirds: controlling junction chirality and polarity in 3D DNA tiles, *Small*, 2023, **19**, 1–8.
31 C. Pigliacelli, K. B. Sanjeeva Nonappa, A. Pizzi, A. Gori, F. B. Bombelli and P. Metrangolo, In situ generation of chiroptically-active gold-peptide superstructures promoted by iodination, *ACS Nano*, 2019, **13**, 2158–2166.
32 P. De Gauquier, K. Vanommeslaeghe, Y. Vander Heyden and D. Mangelings, Modelling approaches for chiral chromatography on polysaccharidebased and macrocyclic antibiotic chiral selectors: A review, *Anal. Chim. Acta*, 2022, **1198**, 1–16.
33 S. Horvátha, Z. Eke and G. Németh, A protocol to replace dedication to either normal phase or polar organic mode for chiral stationary phases containing amylose tris(3,5-dimethylphenylcarbamate), *J. Chromatogr. A*, 2022, **1673**, 1–12.
34 Y. Wang, J. K. Chen, L. X. Xiong, B. J. Wang, S. M. Xie, J. H. Zhang and L. M. Yuan, Preparation of novel chiral stationary phases based on the chiral porous organic cage by thiol-ene click chemistry for enantioseparation in HPLC, *Anal. Chem.*, 2022, **94**, 4961–4969.
35 D. Li, L. Sun, Y. Ding, M. Liu, L. Xie, Y. Liu, L. Shang, Y. Wu, H. Jiang, L. Chi, X. Qiu and W. Xu, Water-induced chiral separation on a Au(111) surface, *ACS Nano*, 2021, **15**, 16896–16903.
36 F. Feng, S. Zhang, L. Yang, G. Li, W. Xu, H. Qu, J. Zhang, M. K. Dhinakaran, C. Xu, J. Cheng and H. Li, Highly chiral selective resolution in pillar[6]arenes functionalized microchannel membranes, *Anal. Chem.*, 2022, **94**, 6065–6070.
37 C. Fanali, Enantiomers separation by capillary electrochromatography, *Trends Anal. Chem.*, 2019, **120**, 115640.

38 T. Hong, X. Liu, Q. Zhou, Y. Liu, J. Guo, W. Zhou, S. Tan and Z. Cai, What the microscale systems 'see' in biological assemblies: cells and viruses?, *Anal. Chem.*, 2022, **94**, 59–74.
39 Z. Feng, Y. Yang, G. Xu, Y. Du and X. Sun, Investigation of the synergistic effect with chiral D-penicillamine functionalized gold nanoparticle as an additive for enantiomeric separation in capillary electrophoresis, *Electrophoresis*, 2020, **41**, 1060–1066.
40 L. F. Hu, S. J. Yin, H. Zhang and F. Q. Yang, Recent developments of monolithic and open-tubular capillary electrochromatography (2017-2019), *J. Sep. Sci.*, 2020, **43**, 1942–1966.
41 C. Chen, W. Liu and T. Hong, Novel approaches for biomolecules immobilization in microscale systems, *Analyst*, 2019, **144**, 3912–3924.
42 M. Greño, M. L. Marina and M. Castro-Puyana, Use of single and dual systems of γ-cyclodextrin or γ-cyclodextrin/L-Carnitine derived ionic liquid for the enantiomeric determination of cysteine by electrokinetic chromatography. A comparative study, *Microchem. J.*, 2021, **169**, 106596.
43 F. Oukacine, C. Ravelet and E. Peyrin, Enantiomeric sensing and separation by nucleic acids, *Trends Anal. Chem.*, 2020, **122**, 115733.
44 M. Greño, M. Castro-Puyana and M. L. Marina, Enantiomeric separation of homocysteine and cysteine by electrokinetic chromatography using mixtures of γ-cyclodextrin and carnitine-based ionic liquids, *Microchem. J.*, 2020, **157**, 105070.
45 Z. Yang, Y. Wei, J. Wei and Z. Yang, Chiral superstructures of inorganic nanorods by macroscopic mechanical grinding, *Nat. Commun.*, 2022, **13**, 1–11.
46 W. Heyvaert, A. Pedrazo-Tardajos, A. Kadu, N. Claes, G. González-Rubio, L. M. Liz-Marzán, W. Albrecht and S. Bals, Quantification of the helical morphology of chiral gold nanorods, *ACS Mater. Lett.*, 2022, **4**, 642–649.
47 Y. Zhao, Y. Zhang, H. Liu and B. Sun, A visual chiroptical system with chiral assembly graphene quantum dots for D-phenylalanine detection, *Anal. Bioanal. Chem.*, 2022, **414**, 4885–4896.
48 N. Dong, Y. Sun, G. Sun, L. Zhang and S. Sun, Chiral DNA nanotubes self-assembled from building blocks with tailorable curvature and twist, *Small*, 2022, **18**, 1–9.
49 A. Carone, P. Mariani, A. Désert, M. Romanelli, J. Marcheselli, M. Garavelli, S. Corni, I. Rivalta and S. Parola, Insight on chirality encoding from small thiolated molecule to plasmonic Au@Ag and Au@Au nanoparticles, *ACS Nano*, 2022, **16**, 1089–1101.
50 N. Kowalska, F. Bandalewicz, J. Kowalski, S. Gómez-Graña, M. Baginski, I. Pastoriza-Santos, M. Grzelczak, J. Matraszek, J. Pérez-Juste and W. Lewandowski, Hydrophobic gold nanoparticles with intrinsic chirality for the efficient fabrication of chiral plasmonic nanocomposites, *ACS Appl. Mater. Interfaces*, 2022, **14**, 50013–50023.
51 G. Zheng, S. Jiao, W. Zhang, S. Wang, Q. Zhang, L. Gu, W. Ye, J. Li, X. Ren, Z. Zhang and K. Wong, Fine-tune chiroptical activity in discrete chiral Au nanorods, *Nano Res.*, 2022, **15**, 6574–6581.
52 M. Ji, Z. Zhou, W. Cao, N. Ma, W. Xu and Y. Tian, A universal way to enrich the nanoparticle lattices with polychrome DNA origami 'homologs', *Sci. Adv.*, 2022, **8**, 1–9.
53 G. A. Knappe, E. C. Wamhoff and M. Bathe, Functionalizing DNA origami to investigate and interact with biological systems, *Nat. Rev. Mater.*, 2023, **8**, 123–138.
54 J. Zou, A. C. Stammers, A. Taladriz-Sender, J. M. Withers, I. Christie, M. S. Vega, B. L. Aekbote, W. J. Peveler, D. A. Rusling, G. A. Burley and A. W. Clark, Fluorous-directed assembly of DNA origami nanostructures, *ACS Nano*, 2023, **17**, 752–759.
55 X. Wang, Z. Mao, R. Chen, S. Li, S. Ren, J. Liang and Z. Gao, Self-assembled DNA origami-based duplexed aptasensors combined with centrifugal filters for efficient and rechargeable ATP detection, *Biosens. Bioelectron.*, 2022, **211**, 114336.
56 L. M. Kneer, E. Roller, L. V. Besteiro, R. Schreiber, A. O. Govorov and T. Liedl, Circular dichroism of chiral molecules in DNA assembled plasmonic hotspots, *ACS Nano*, 2018, **12**, 9110–9115.
57 A. Kuzyk, M. J. Urban, A. Idili, F. Ricci and N. Liu, Selective control of reconfigurable chiral plasmonic metamolecules, *Sci. Adv.*, 2017, **3**, 1602803.
58 K. Martens, F. Binkowski, L. Nguyen, L. Hu, A. O. Govorov, S. Burger and T. Liedl, Long- and short-ranged chiral interactions in DNA-assembled plasmonic chains, *Nat. Commun.*, 2021, **12**, 2025.
59 T. Funck, F. Nicoli, A. Kuzyk and T. Liedl, Sensing picomolar concentrations of RNA using switchable plasmonic chirality, *Angew. Chem.*, 2018, **57**, 13495–13498.
60 O. Ávalos-Ovando, L. V. Besteiro, A. Movsesyan, G. Markovich, T. Liedl, K. Martens, Z. Wang, M. A. Correa-Duarte and A. O. Govorov, Chiral photomelting of DNA-nanocrystal assemblies utilizing plasmonic photoheating, *Nano Lett.*, 2021, **21**, 7298–7308.
61 Q. Jiang, Q. Liu, Y. Shi, Z. Wang, P. Zhan, J. Liu, C. Liu, H. Wang, X. Shi, L. Zhang, J. Sun, B. Ding and M. Liu, Stimulus-responsive plasmonic chiral signals of gold nanorods organized on DNA origami, *Nano Lett.*, 2017, **17**, 7125–7130.
62 B. Shen, V. Linko, K. Tapio, S. Pikker, T. Lemma, A. Gopinath, K. V. Gothelf, M. A. Kostiainen and J. J. Toppari, Plasmonic nanostructures through DNA-assisted lithography, *Sci. Adv.*, 2018, **4**, eaap8978.
63 M. M. C. Tortora, G. Mishra, D. Prešern and J. P. K. Doye, Chiral shape fluctuations and the origin of chirality in cholesteric phases of DNA origamis, *Sci. Adv.*, 2020, **6**, eaaw8331.
64 M. Nguyen and A. Kuzyk, Reconfigurable chiral plasmonics beyond single chiral centers, *ACS Nano*, 2019, **13**, 13615–13619.
65 L. Nguyen, M. Dass, M. F. Ober, L. V. Besteiro, Z. M. Wang, B. Nickel, A. O. Govorov, T. Liedl and A. Heuer-Jungemann,

Chiral assembly of gold-silver core-shell plasmonic nanorods on DNA origami with strong optical activity, *ACS Nano*, 2020, **14**, 7454–7461.

66 Q. Jiang, X. Xu, P. Yin, K. Ma, Y. Zhen, P. Duan, Q. Peng, W. Q. Chen and B. Ding, Circularly polarized luminescence of achiral cyanine molecules assembled on DNA templates, *J. Am. Chem. Soc.*, 2019, **141**, 9490–9494.

67 J. Gong and X. Zhang, Coordination-based circularly polarized luminescence emitters: Design strategy and application in sensing, *Coordin. Chem. Rev.*, 2022, **453**, 214329.

68 Y. Huang, M. Nguyen, A. K. Natarajan, V. H. Nguyen and A. Kuzyk, A DNA origami-based chiral plasmonic sensing device, *ACS Appl. Mater. Interfaces*, 2018, **10**, 44221–44225.

69 B. Chovelon, E. Fiorea, P. Faure, E. Peyrina and C. Ravelet, Kissing interactions for the design of a multicolour fluorescence anisotropy chiral aptasensor, *Talanta*, 2019, **205**, 120098.

70 Y. Huang, M. Nguyen, V. H. Nguyen, J. Loo, A. J. Lehtonen and A. Kuzyk, Characterizing aptamers with reconfigurable chiral plasmonic assemblies, *Langmuir*, 2022, **38**, 2954–2960.

71 Y. Huang, J. Ryssy, M. Nguyen, J. Loo, S. Hällsten and A. Kuzyk, Measuring the affinities of RNA and DNA aptamers with DNA origami-based chiral plasmonic probes, *Anal. Chem.*, 2022, **94**, 17577–17586.

72 G. Xu, J. Zhao, H. Yu, C. Wang, Y. Huang, Q. Zhao, X. Zhou, C. Li and M. Liu, Structural insights into the mechanism of high-affinity binding of ochratoxin A by a DNA aptamer, *J. Am. Chem. Soc.*, 2022, **144**, 7731–7740.

73 J. Cai, C. Hao, M. Sun, W. Ma, C. Xu and H. Kuang, Chiral shell core-satellite nanostructures for ultrasensitive detection of mycotoxin, *Small*, 2018, **14**, 1703931.

74 Y. Hu, F. Lin, T. Wu, Y. Zhou, Q. Li, Y. Shao and Z. Xu, DNA duplex engineering for enantioselective fluorescent sensor, *Anal. Chem.*, 2017, **89**, 2181–2185.

75 C. Zhao, H. Song, P. Scott, A. Zhao, H. Tateishi-Karimata, N. Sugimoto, J. Ren and X. Qu, Mirror-image dependence: targeting enantiomeric G-quadruplex DNA using triplex metallohelices, *Angew. Chem.*, 2018, **130**, 15949–15953.

76 M. Golla, S. K. Albert, S. Atchimnaidu, D. Perumal, N. Krishnan and R. Varghese, DNA-decorated, helically twisted nanoribbons: a scaffold for the fabrication of one-dimensional, chiral, plasmonic nanostructures, *Angew. Chem., Int. Ed.*, 2019, **58**, 3865–3869.

77 X. Lan, Z. Su, Y. Zhou, T. Meyer, Y. Ke, Q. Wang, W. Chiu, N. Liu, S. Zou, H. Yan and Y. Liu, Programmable supraassembly of a DNA surface adapter for tunable chiral directional self-assembly of gold nanorods, *Angew. Chem.*, 2017, **129**, 14824–14828.

78 M. Balaz, T. Shambhavi and V. Krisztina, Chiral multichromophoric supramolecular nanostructures assembled by single stranded DNA and RNA templates, *Coordin. Chem. Rev.*, 2017, **349**, 66–83.

79 B. Liu, L. Han and S. Che, Formation of enantiomeric impeller-like helical architectures by DNA self-assembly and silica mineralization, *Angew. Chem. Int. Ed.*, 2012, **51**, 923–927.

80 S. S. M. Ameen, N. M. S. Mohammed and K. M. Omer, Ultra-small highly fluorescent zinc-based metal organic framework nanodots for ratiometric visual sensing of tetracycline based on aggregation induced emission, *Talanta*, 2023, **254**, 124178.

81 C. Chen, H. Xu, Q. Zhan, Y. Zhang, B. Wang, C. Chen, H. Tang and Q. Xie, Preparation of novel HKUST-1glucose oxidase composites and their application in biosensing, *Microchim. Acta*, 2023, **190**, 1–10.

82 T. Huang, M. Wang, N. Hong, H. Cui, Q. Fan, G. Wei, L. Qin, J. Zhang and H. Fan, An autonomous driven DNA walker-based electrochemical aptasensor for on-site detection of Ochratoxin A, *Talanta*, 2023, **252**, 123785.

83 H. Li, H. Shi, X. Chen, Z. Ren, Y. Shen, P. Wu, Y. Fan, X. Zhang, W. Shi, H. Liao, S. Zhang, W. Zhang and F. Huo, Construction of metal-organic framework films *via* crosslinking-induced assembly, *Adv. Mater.*, 2023, **35**, 2209777.

84 M. Liu, L. Zu and Z. M. Hudson, Mechanistic principles for engineering hierarchical porous metal-organic frameworks, *ACS Nano*, 2022, **16**, 13573–13594.

85 D. Wu, L. Tan, C. Ma, F. Pan, W. Cai, J. Li and Y. Kong, Competitive self-assembly interaction between ferrocenyl units and amino acids for entry into the cavity of β-cyclodextrin for chiral electroanalysis, *Anal. Chem.*, 2022, **94**, 6050–6056.

86 A. Wang, K. Liu, M. Tian and L. Yang, Open tubular capillary electrochromatography-mass spectrometry for analysis of underivatized amino acid enantiomers with a porous layer-gold nanoparticle-modified chiral column, *Anal. Chem.*, 2022, **94**, 9252–9260.

87 Y. W. Zhao, Y. Wang and X. M. Zhang, Homochiral MOF as circular dichroism sensor for enantioselective recognition on nature and chirality of unmodified amino acids, *ACS Appl. Mater. Interfaces*, 2017, **9**, 20991–20999.

88 M. W. Rahman, K. M. Alam and S. Pramanik, Long carbon nanotubes functionalized with DNA and implications for spintronics, *ACS Omega*, 2018, **3**, 17108–17115.

89 W. He, J. Dai, T. Li, Y. Bao, F. Yang, X. Zhang and H. Uyama, Novel strategy for the investigation on chirality selection of single walled carbon nanotubes with DNA by electrochemical characterization, *Anal. Chem.*, 2018, **90**, 12810–12814.

90 L. Zhang, J. Gao, K. Luo, J. Li and Y. Zeng, Protein synergistic action-based development and application of a molecularly imprinted chiral sensor for highly stereoselective recognition of S-fluoxetine, *Biosens. Bioelectron.*, 2023, **223**, 1–5.

91 Y. Sun, S. Wang, Y. Sheng, R. Zhang, D. Xu and M. Bradley, Construction of CS/BSA multilayers for electrochemical recognition of tryptophan enantiomers, *J. Electroanal. Chem.*, 2022, **923**, 1–9.

92 H. Pei, J. Wang, X. Jin, X. Zhang, W. Liu, R. Guo, N. Liu and Z. Mo, An electrochemical chiral sensor based on glutamic acid functionalized graphene-gold nanocomposites for chiral recognition of tryptophan enantiomers, *J. Electroanal. Chem.*, 2022, **913**, 1–12.

93 Y. Deng, Z. Zhang, Y. Pang, X. Zhou, Y. Wang, Y. Zhang and Y. Yuan, Common materials, extraordinary behavior: an ultrasensitive and enantioselective strategy for D-tryptophan recognition based on electrochemical Au@p-L-cysteine chiral interface, *Anal. Chim. Acta*, 2022, **1227**, 1–10.
94 Q. Ye, L. Guo, D. Wu, B. Yang, Y. Tao, L. Deng and Y. Kong, Covalent functionalization of bovine serum albumin with graphene quantum dots for stereospecific molecular recognition, *Anal. Chem.*, 2019, **91**, 11864–11871.
95 R. Malishev, E. Arad, S. K. Bhunia, S. Shaham-Niv, S. Kolusheva, E. Gazit and R. Jelinek, Chiral modulation of amyloid beta fibrillation and cytotoxicity by enantiomeric carbon dots, *Chem. Commun.*, 2018, **54**, 7762–7765.
96 C. Pang, N. Zhang and M. Falahati, Acceleration of α-synuclein fibril formation and associated cytotoxicity stimulated by silica nanoparticles as a model of neurodegenerative diseases, *Int. J. Biol. Macromol.*, 2021, **169**, 532–540.
97 L. Wang, W. Gao, S. Ng and M. Pumera, Chiral protein-covalent organic framework 3D-printed structures as chiral biosensors, *Anal. Chem.*, 2021, **93**, 5277–5283.
98 Q. Zhang, T. Hernandez, K. W. Smith, S. A. H. Jebeli, A. X. Dai, L. Warning, R. Baiyasi, L. A. McCarthy, H. Guo, D. Chen, J. A. Dionne, C. F. Landes and S. Link, Unraveling the origin of chirality from plasmonic nanoparticle-protein complexes, *Science*, 2019, **365**, 1475–1478.
99 J. Kim and N. A. Kotov, Origin of chiroptical activity in nanorod assemblies, *Science*, 2019, **27**, 1378–1379.
100 Y. Kim, B. Yeom, O. Arteaga, S. Jo Yoo, S. G. Lee, J. G. Kim and N. A. Kotov, Reconfigurable chiroptical nanocomposites with chirality transfer from the macro- to the nanoscale, *Nat. Mater.*, 2016, **15**, 461–468.
101 R. Tullius, A. S. Karimullah, M. Rodier, B. Fitzpatrick, N. Gadegaard, L. D. Barron, V. M. Rotello, G. Cooke, A. Lapthorn and M. Kadodwala, Superchiral spectroscopy: detection of protein higher order hierarchical structure with chiral plasmonic nanostructures, *J. Am. Chem. Soc.*, 2015, **137**, 8380–8383.
102 Y. Zhang, X. Liu, S. Qiu, Q. Zhang, W. Tang, H. Liu, Y. Guo, Y. Ma, X. Guo and Y. Liu, A flexible acetylcholinesterase-modified graphene for chiral pesticide sensor, *J. Am. Chem. Soc.*, 2019, **141**, 14643–14649.
103 S. Wu, Q. He, C. Tan, Y. Wang and H. Zhang, Graphene-based electrochemical sensors, *Small*, 2013, **9**, 1121–1410.
104 Y. Zhao, X. Li, X. Zhou and Y. Zhang, Review on the graphene based optical fiber chemical and biological sensors, *Sens. Actuators, B*, 2016, **231**, 324–340.
105 M. L. Verma, S. B. S. Dhanya, R. Saini, A. Das and R. S. Varma, Synthesis and application of graphene-based sensors in biology: a review, *Environ. Chem. Lett.*, 2022, **20**, 2189–2212.
106 Y. Liu, X. Dong and P. Chen, Biological and chemical sensors based on graphene materials, *Chem. Soc. Rev.*, 2012, **41**, 2283–2307.
107 A. Nag, A. Mitra and S. C. Mukhopadhyay, Graphene and its sensor-based applications: A review, *Sens. Actuators, A*, 2018, **270**, 177–194.
108 H. Liu, J. Shao, L. Shi, W. Ke, F. Zheng and Y. Zhao, Electroactive NPs and D-amino acids oxidase engineered electrochemical chiral sensor for D-alanine detection, *Sens. Actuators, B*, 2020, **304**, 127333.
109 M. Sun, S. Peng, L. Nie, Y. Zou, L. Yang, L. Gao, X. Dou, C. Zhao and C. Feng, Three-dimensional chiral supramolecular microenvironment strategy for enhanced biocatalysis, *ACS Nano*, 2021, **15**, 14972–14984.
110 J. Luo, Y. Cheng, Z. Gong, K. Wu, Y. Zhou, H. Chen, M. Gauthier, Y. Cheng, J. Liang and T. Zou, Self-assembled peptide functionalized gold nanopolyhedrons with excellent chiral optical properties, *Langmuir*, 2020, **36**, 600–608.
111 G. Gonzalez-Rubio and L. M. Marzan, A peptide-guided twist of light, *Nature*, 2018, **556**, 313–314.
112 H. Lee, H. Ahn, J. Mun, Y. Y. Lee, M. Kim, N. H. Cho, K. Chang, W. S. Kim, J. Rho and K. T. Nam, Amino-acid- and peptide-directed synthesis of chiral plasmonic gold nanoparticles, *Nature*, 2018, **556**, 360–365.
113 R. Jurado, J. Adamcik, M. Lopez-Haro, J. A. Gonzalez-Vera, A. Ruiz-Arias, A. Sanchez-Ferrer, R. Cuesta, J. M. Domínguez-Vera, J. J. Calvino, A. Orte, R. Mezzenga and N. Galvez, Apoferritin protein amyloid fibrils with tunable chirality and polymorphism, *J. Am. Chem. Soc.*, 2019, **141**, 1606–1613.
114 K. T. Nam and H. Kim, Gold meets peptides in a hybrid coil, *Science*, 2021, **371**, 1311.
115 J. Lu, Y. Xue, K. Bernardino, N. Zhang, W. R. Gomes, N. S. Ramesar, S. Liu, Z. Hu, T. Sun, A. F. de Moura, N. A. Kotov and K. Liu, Enhanced optical asymmetry in supramolecular chiroplasmonic assemblies with long-range order, *Science*, 2021, **371**, 1368–1374.
116 H. Kim, K. Bang, H. Ha, N. H. Cho, S. D. Namgung, S. W. Im, K. H. Cho, R. M. Kim, W. I. Choi, Y. Lim, J. Shin, H. K. Song, N. Kim and K. T. Nam, Tyrosyltyrosylcysteine-directed synthesis of chiral cobalt oxide nanoparticles and peptide conformation analysis, *ACS Nano*, 2021, **15**, 979–988.
117 A. Sanchez-Ferrer, J. Adamcik, S. Handschin, S. H. Hiew, A. Miserez and R. Mezzenga, Controlling supramolecular chiral nanostructures by self-assembly of a biomimetic β-sheet-rich amyloidogenic peptide, *ACS Nano*, 2018, **12**, 9152–9161.
118 K. Hu, Y. Jiang, W. Xiong, H. Li, P. Zhang, F. Yin, Q. Zhang, H. Geng, F. Jiang, Z. Li, X. Wang and Z. Li, Tuning peptide self-assembly by an in-tether chiral center, *Sci. Adv.*, 2018, **4**, 1–8.
119 X. Yang, Y. Shen, J. Liu, Y. Wang, W. Qi, R. Su and Z. He, Rational design of chiral nanohelices from self-assembly of mesotetrakis (4-carboxyphenyl) porphyrin-amino acid conjugates, *Langmuir*, 2021, **37**, 13067–13074.
120 Y. Fan, Q. Xing, J. Zhang, Y. Wang, Y. Liang, W. Qi, R. Su and Z. He, Self-assembly of peptide chiral nanostructures with sequence encoded enantioseparation capability, *Langmuir*, 2020, **36**, 10361–10370.
121 Q. Ye, Z. Yin, H. Wu, D. Wu, Y. Tao and Y. Kong, Decoration of glutathione with copper-platinum nanoparticles for

chirality sensing of tyrosine enantiomers, *Electrochem. Commun.*, 2020, **110**, 106638.

122 C. Furman, M. Howsam and E. Lipka, Recent developments in separation methods for enantiomeric ratio determination of amino acids specifically involved in cataract and Alzheimer's disease, *Trends Anal. Chem.*, 2021, **141**, 1–12.

123 Q. Cheng, H. Pei, Q. Ma, R. Guo, N. Liu and Z. Mo, Chiral graphene materials for enantiomer separation, *Chem. Eng. J.*, 2023, **452**, 1–25.

124 Q. Cheng, Q. Ma, H. Pei and Z. Mo, Chiral membranes for enantiomer separation: A comprehensive review, *Sep. Purif. Technol.*, 2022, **292**, 1–13.

125 X. Fan, L. Cao, L. Geng, Y. Ma, Y. Wei and Y. Wang, Polysaccharides as separation media for the separation of proteins, peptides and stereoisomers of amino acids, *Int. J. Biol. Macromol.*, 2021, **186**, 616–638.

126 S. Xie, X. Chen, J. Zhang and L. Yuan, Gas chromatographic separation of enantiomers on novel chiral stationary phases, *Trends Anal. Chem.*, 2020, **124**, 1–20.

127 F. Feizi, M. Shamsipur, A. Barati, M. B. Gholivand and F. Mousavi, Chiral recognition and quantitative analysis of tyrosine enantiomers using L-cysteine capped CdTe quantum dots: Circular dichroism, fluorescence, and theoretical calculation studies, *Microchem. J.*, 2020, **158**, 105168.

128 H. Zhang, H. He, X. Jiang, Z. Xia and W. Wei, Preparation and characterization of chiral transition-metal dichalcogenide quantum dots and their enantioselective catalysis, *ACS Appl. Mater. Interfaces*, 2018, **10**, 30680–30688.

129 X. Mao, Z. Wang, D. Zeng, H. Cao, Y. Zhan, Y. Wang, Q. Li, Y. Shen and J. Wang, Self-assembled chiral nanoparticle superstructures and identification of their collective optical activity from ligand asymmetry, *ACS Nano*, 2019, **13**, 2879–2887.

130 Q. Zhang, M. Fu, H. Lu, X. Fan, H. Wang, Y. Zhang and H. Wang, Novel potential and current type chiral amino acids biosensor based on L/D-handed double helix carbon nanotubes@polypyrrole@Au nanoparticles@L/D-cysteine, *Sens. Actuators, B*, 2019, **296**, 126667.

131 D. Suttipat, S. Butcha, S. Assavapanumat, T. Maihom, B. Gupta, A. Perro, N. Sojic, A. Kuhn and C. Wattanakit, Chiral macroporous MOF surfaces for electroassisted enantioselective adsorption and separation, *ACS Appl. Mater. Interfaces*, 2020, **12**, 36548–36557.

132 F. Zhu, J. Wang, S. Xie, Y. Zhu, L. Wang, J. Xu, S. Liao, J. Ren, Q. Liu, H. Yang and X. Chen, L-pyroglutamic acid-modified CdSe/ZnS quantum dots: a new fluorescence-responsive chiral sensing platform for stereospecific molecular recognition, *Anal. Chem.*, 2020, **92**, 12040–12048.

133 S. Wu, Z. Yin, D. Wu, Y. Tao and Y. Kong, Chiral enantioselective assemblies induced from achiral porphyrin by L- and D-lysine, *Langmuir*, 2019, **35**, 16761–16769.

134 K. Chen, T. Jiao, J. Li, D. Han, R. Wang, G. Tian and Q. Peng, Chiral nanostructured composite films *via* solvent-tuned self assembly and their enantioselective performances, *Langmuir*, 2019, **35**, 3337–3345.

135 P. Xing, Y. Li, S. Xue, S. Z. F. Phua, C. Ding, H. Chen and Y. Zhao, Occurrence of chiral nanostructures induced by multiple hydrogen bonds, *J. Am. Chem. Soc.*, 2019, **141**, 9946–9954.

136 C. S. Ong, J. Z. Oor, S. J. Tan and J. W. Chew, Enantiomeric separation of racemic mixtures using chiral-selective and organic-solvent-resistant thin-film composite membranes, *ACS Appl. Mater. Interfaces*, 2022, **14**, 10875–10885.

137 D. Ujj, E. Kalydi, M. Malanga, E. Varga, T. Sohajda, S. Béni and G. Benkovics, Sugammadex analogue cyclodextrins as chiral selectors for enantioseparation of cathinone derivatives by capillary electrophoresis, *J. Chromatogr. A*, 2022, **1683**, 1–12.

138 W. Tang, Y. Lu, K. H. Row, S. H. Baeck, Y. Zhang and G. Sun, Novel bovine serum album and β-cyclodextrin-based mixed chiral stationary phase for the enantioseparation in capillary electrochromatography, *Microchem. J.*, 2022, **181**, 1–8.

139 W. Sun, B. Chen, H. You, L. Fang, J. Qian and S. Tong, Enantioseparation of N-methyl duloxetine, duloxetine, and fluoxetine by countercurrent chromatography using anionic β-cyclodextrin as chiral selector, *J. Sep. Sci.*, 2022, **45**, 3022–3030.

140 X. Lu, M. Chen, J. Yang, M. Zhang, Y. Li and Y. Wang, Surface-up construction of quinine bridged functional cyclodextrin for single-column versatile enantioseparation, *J. Chromatogr. A*, 2022, **1664**, 1–9.

141 J. Zou, G. Zhao, J. Guan, X. Jiang and J. Yu, Single-layer graphene oxide-amino-β-cyclodextrin/black phosphorus nanosheet composites for recognition of tyrosine enantiomers, *ACS Appl. Nano Mater.*, 2021, **4**, 13329–13338.

142 X. Niu, X. Yang, Z. Mo, R. Guo, N. Liu, P. Zhao and Z. Liu, Perylene-functionalized graphene sheets modified with β-cyclodextrin for the voltammetric discrimination of phenylalanine enantiomers, *Bioelectrochemistry*, 2019, **129**, 189–198.

143 X. Niu, Z. Mo, X. Yang, C. Shuai, N. Liu and R. Guo, Graphene-ferrocene functionalized cyclodextrin composite with high electrochemical recognition capability for phenylalanine enantiomers, *Bioelectrochemistry*, 2019, **128**, 74–82.

144 X. Niu, X. Yang, Z. Mo, N. Liu, R. Guo, Z. Pan and Z. Liu, Electrochemical chiral sensing of tryptophan enantiomers by using 3D nitrogen-doped reduced graphene oxide and self-assembled polysaccharides, *Microchim. Acta*, 2019, **186**, 1–12.

145 D. Wu and Y. Kong, Dynamic interaction between host and guest for enantioselective recognition: application of β-cyclodextrin-based charged catenane as electrochemical probe, *Anal. Chem.*, 2019, **91**, 5961–5967.

146 Y. Chen, S. Pangannaya, B. Sun, C. Qian, G. Sun, M. Cheng, C. Lin, X. Lu, J. Jiang and L. Wang, Stoichiometry-controlled chirality induced by co-assembly of tetraphenylethylene derivative, γ-CD, and water-soluble pillar[5]-arene, *ACS Appl. Bio Mater.*, 2021, **4**, 2066–2072.

147 R. R. Poolakkandy, A. R. Neelakandan, K. A. Padmalayam, G. K. Rajanikant and M. M. Menamparambath, Nickel

hydroxide nanoflake/carbon nanotube composites for the electrochemical detection of glutamic acid using In vitro stroke model, *ACS Appl. Nano Mater.*, 2023, **6**, 1347–1359.
148 M. Aminikhah, A. Babaei and A. Taheri, A novel electrochemical sensor based on molecularly imprinted polymer nanocomposite platform for sensitive and ultra-selective determination of citalopram, *J. Electroanal. Chem.*, 2022, **918**, 1–11.
149 Ö. S. Bölükbaşı, B. B. Yola, H. Boyacıoğlu and M. L. Yola, A novel paraoxon imprinted electrochemical sensor based on MoS_2NPs@MWCNTs and its application to tap water samples, *Food Chem. Toxicol.*, 2022, **163**, 1–8.
150 H. Zhao, K. Shi, C. Zhang, J. Ren, M. Cui, N. Li, X. Ji and R. Wang, Spherical COFs decorated with gold nanoparticles and multiwalled carbon nanotubes as signal amplifier for sensitive electrochemical detection of doxorubicin, *Microchem. J.*, 2022, **182**, 1–9.
151 J. N. Tiwari, V. Vij, K. C. Kemp and K. S. Kim, Engineered carbon-nanomaterial-based electrochemical sensors for biomolecules, *ACS Nano*, 2016, **10**, 46–80.
152 X. Niu, X. Yang, Z. Mo, R. Guo, N. Liu, P. Zhao, Z. Liu and M. Ouyang, Voltammetric enantiomeric differentiation of tryptophan by using multiwalled carbon nanotubes functionalized with ferrocene and β-cyclodextrin, *Electrochim. Acta*, 2019, **297**, 650–659.
153 S. S. Upadhyay and A. K. Srivastava, Hydroxypropyl β-cyclodextrin cross-linked multiwalled carbon nanotube-based chiral nanocomposite electrochemical sensors for the discrimination of multichiral drug atorvastatin isomers, *New J. Chem.*, 2019, **43**, 11178–11188.
154 P. Lei, Y. Zhou, G. Zhang, Y. Zhang, C. Zhang, S. Hong, Y. Yang, C. Dong and S. Shuang, A highly efficient chiral sensing platform for tryptophan isomers based on a coordination self-assembly, *Talanta*, 2019, **195**, 306–312.
155 J. Song, C. Yang, J. Ma, Q. Han, P. Ran and Y. Fu, Voltammetric chiral discrimination of tryptophan using a multilayer nanocomposite with implemented amino-modified β-cyclodextrin as recognition element, *Microchim. Acta*, 2018, 1–9.
156 F. Li, F. Wu, X. Luan, Y. Yuan, L. Zhang, G. Xu and W. Niu, Highly enantioselective electrochemical sensing based on helicoid Au nanoparticles with intrinsic chirality, *Sens. Actuators, B*, 2022, **362**, 1–8.
157 E. Zor, H. Bingol and M. Ersoz, Chiral sensors, *Trends Anal. Chem.*, 2019, **121**, 1–17.
158 Y. Yang, M. Li and Z. Zhu, A disposable dual-signal enantioselective electrochemical sensor based on stereogenic porous chiral carbon nanotubes hydrogel, *Talanta*, 2021, **232**, 1–8.
159 M. P. Tiwari and A. Prasad, Molecularly imprinted polymer based enantioselective sensing devices: A review, *Anal. Chim. Acta*, 2015, **853**, 1–18.
160 J. Zou, G. Zhao, G. Zhao and J. Yu, Fast and sensitive recognition of enantiomers by electrochemical chiral analysis: Recent advances and future perspectives, *Coordin. Chem. Rev.*, 2022, **471**, 1–24.
161 S. S. Upadhyay, N. S. Gadhari and A. K. Srivastava, Biomimetic sensor for ethambutol employing β-cyclodextrin mediated chiral copper metal organic framework and carbon nanofibers modified glassy carbon electrode, *Biosens. Bioelectron.*, 2020, **165**, 1–5.
162 J. Zou and J. Yu, Nafion-stabilized black phosphorus nanosheets-maltosyl-β-cyclodextrin as a chiral sensor for tryptophan enantiomers, *Mater. Sci. Eng., C*, 2020, **112**, 110910.
163 J. Zou, X. Lan, G. Zhao, Z. Huang, Y. Liu and J. Yu, Immobilization of 6-O-α-maltosyl-β-cyclodextrin on the surface of black phosphorus nanosheets for selective chiral recognition of tyrosine enantiomers, *Microchim. Acta*, 2020, **187**, 1–11.
164 J. Liu, B. Fu and Z. Zhang, Ionic current rectification triggered photoelectrochemical chiral sensing platform for recognition of amino acid enantiomers on self-standing nanochannel arrays, *Anal. Chem.*, 2020, **92**, 8670–8674.
165 Y. Luo, X. Zhao, P. Cai and Y. Pan, One-pot synthesis of an anionic cyclodextrin-stabilized bifunctional gold nanoparticles for visual chiral sensing and catalytic reduction, *Carbohyd. Polym.*, 2020, **237**, 1–9.
166 Y. Gao, W. Chen and Z. Bai, Requirements in structure for chiral recognition of chitosan derivatives, *J. Chromatogr. A*, 2023, **1690**, 1–12.
167 W. Chen, J. Jianga, G. Qiu, S. Tang and Z. Bai, The interactions between chiral analytes and chitosan-based chiral stationary phases during enantioseparation, *J. Chromatogr. A*, 2021, **1650**, 1–11.
168 G. Zhang, J. Xi, W. Chen and Z. Bai, Comparison in enantioseparation performance of chiral stationaryphases prepared from chitosans of different sources and molecular weights, *J. Chromatogr. A*, 2020, **1621**, 1–9.
169 L. Zhang, H. Deng, X. Wu, H. Gao, J. Shen, H. Cao, Y. Qiao and Y. Okamoto, Enantioseparation using chitosan 2-isopropylthiourea-3,6-dicarbamate derivatives as chiral stationary phases for high-performance liquid chromatography, *J. Chromatogr. A*, 2020, **1623**, 1–9.
170 P. Peluso and B. Chankvetadze, Native and substituted cyclodextrins as chiral selectors for capillary electrophoresis enantioseparations: Structures, features, application, and molecular modeling, *Electrophoresis*, 2021, **42**, 1676–1708.
171 X. Yang, X. Niu, Z. Mo, R. Guo, N. Liu, P. Zhao and Z. Liu, Perylene-functionalized graphene sheets modified with chitosan for voltammetric discrimination of tryptophan enantiomers, *Microchim. Acta*, 2019, **186**, 1–12.
172 X. Niu, X. Yang, Z. Mo, J. Wang, Z. Pan, Z. Liu, C. Shuai, G. Liu, N. Liu and R. Guo, Fabrication of an electrochemical chiral sensor *via* an integrated polysaccharides/3D nitrogen-doped graphene-CNT frame, *Bioelectrochemistry*, 2020, **131**, 1–11.
173 J. Zou, X. Chen, G. Zhao, X. Jiang, F. Jiao and J. Yu, A novel electrochemical chiral interface based on the synergistic effect of polysaccharides for the recognition of tyrosine enantiomers, *Talanta*, 2019, **195**, 628–637.

174 R. A. Zilberg, V. N. Maistrenko, L. R. Kabirova and D. I. Dubrovsky, Selective voltammetric sensors based on composites of chitosan polyelectrolyte complexes with cyclodextrins for recognition and determination of atenolol enantiomers, *Anal. Methods*, 2018, **10**, 1886–1894.

175 R. Xiong, A. Singh, S. Yu, S. Zhang, H. Lee, Y. G. Yingling, D. Nepal, T. J. Bunning and V. V. Tsukruk, Co-assembling polysaccharide nanocrystals and nanofibers for robust chiral iridescent films, *ACS Appl. Mater. Interfaces*, 2020, **12**, 35345–35353.

176 J. Liu, T. Chu, M. Cheng, Y. Su, G. Zou and S. Hou, Bovine serum albumin functional graphene oxide membrane for effective chiral separation, *J. Membr. Sci.*, 2023, **668**, 1–8.

177 S. Amalia, S. C. Angga, E. D. Iftitah, D. Septiana, B. O. D. Anggraeny Warsito, A. N. Hasanah and A. Sabarudin, Immobilization of trypsin onto porous methacrylate-based monolith for flow-through protein digestion and its potential application to chiral separation using liquid chromatography, *Heliyon*, 2021, **7**, 1–11.

178 B. Zhu, M. Xue, B. Liu, Q. Li and X. Guo, Enantioselective separation of eight antihistamines with α_1-acid glycoprotein-based chiral stationary phase by HPLC: Development and validation for the enantiomeric quality control, *J. Pharmaceut. Biomed.*, 2019, **176**, 1–8.

179 Q. Bai, C. Zhang, Y. Zhao, C. Wang, M. Maihemuti, C. Sun, Y. Qi, J. Peng, X. Guo, Z. Zhang and L. Fang, Evaluation of chiral separation based on bovine serum albumin-conjugated carbon nanotubes as stationary phase in capillary electrochromatography, *Electrophoresis*, 2020, **41**, 1253–1260.

180 T. Wang, Y. Wang, Y. Zhang, Y. Cheng, J. Ye, Q. Chu and G. Cheng, Rapid preparation and evaluation of chiral open-tubular columns supported with bovine serum album and zeolite imidazolate framework-8 for mini-capillary electrochromatography, *J. Chromatogr. A*, 2020, **1625**, 1–7.

181 L. Li, X. Xue, H. Zhang, W. Lv, S. Qi, H. Du, A. Manyande and H. Chen, In-situ and one-step preparation of protein film in capillary column for open tubular capillary electrochromatography enantioseparation, *Chinese Chem. Lett.*, 2021, **32**, 2139–2142.

182 W. Ding, T. Yu, Y. Du, X. Sun, Z. Feng, S. Zhao, X. Ma, M. Ma and C. Chen, A metal organic framework-functionalized monolithic column for enantioseparation of six basic chiral drugs by capillary electrochromatography, *Microchim. Acta*, 2020, **187**, 1–10.

183 M. Ma, Y. Du, J. Yang, Z. Feng, W. Ding and C. Chen, Gold nanoparticles-functionalized monolithic column for enantioseparation of eight basic chiral drugs by capillary electrochromatography, *Microchim. Acta*, 2020, **187**, 1–12.

184 M. Ma, C. Chen, X. Zhu, X. Li, Y. Du, L. Zhang and J. Gan, A porous layer open-tubular capillary column supported with pepsin and zeolitic imidazolate framework for enantioseparation of four basic drugs in capillary electrochromatography, *J. Chromatogr. A*, 2021, **1637**, 1–8.

185 Y. Sun, C. Li, X. Niu, C. Pan, H. Zhang, W. Wang, H. Chen and X. Chen, Rapid and mild fabrication of protein membrane coated capillary based on supramolecular assemble for chiral separation in capillary electrochromatography, *Talanta*, 2019, **195**, 190–196.

186 Z. Li, Q. Li, Y. Fu, C. Hu, Y. Liu, W. Li and Z. Chen, A lipase-based chiral stationary phase for direct chiral separation in capillary electrochromatography, *Talanta*, 2021, **233**, 1–7.

187 D. Liu and C. Dong, Recent advances in nano-carrier immobilized enzymes and their applications, *Process Biochem.*, 2020, **92**, 464–475.

188 T. Hong, W. Liu, M. Li and C. Chen, Recent advances in the fabrication and application of nanomaterialbased enzymatic microsystems in chemical and biological sciences, *Anal. Chim. Acta*, 2019, **1067**, 31–47.

189 S. A. Bhakta, E. Evans, T. E. Benavidez and C. D. Garcia, Protein adsorption onto nanomaterials for the development of biosensors and analytical devices: A review, *Anal. Chim. Acta*, 2015, **872**, 7–25.

190 S. Sarkar, K. Gulati, A. Mishra and K. M. Poluri, Protein nanocomposites: special inferences to lysozyme based nanomaterials, *Int. J. Biol. Macromol.*, 2020, **151**, 467–482.

191 O. S. Kwon, H. S. Song, T. H. Park and J. Jang, Conducting nanomaterial sensor using natural receptors, *Chem. Rev.*, 2019, **119**, 36–93.

192 L. Zhou, J. Lun, Y. Liu, Z. Jiang, X. Di and X. Guo, In situ immobilization of sulfated-β-cyclodextrin as stationary phase for capillary electrochromatography enantioseparation, *Talanta*, 2019, **200**, 1–8.

193 L. Pont, G. Marin, M. Vergara-Barberán, L. G. Gagliardi, V. Sanz-Nebot, J. M. Herrero-Martínez and F. Benavente, Polymeric monolithic microcartridges with gold nanoparticles for the analysis of protein biomarkers by on-line solid-phase extraction capillary electrophoresis-mass spectrometry, *J. Chromatogr. A*, 2020, **1622**, 1–8.

194 A. Wang, J. Liu, J. Yang and L. Yang, Aptamer affinity-based microextraction in-line coupled to capillary electrophoresis mass spectrometry using a porous layer/nanoparticle-modified open tubular column, *Anal. Chim. Acta*, 2023, **1239**, 1–8.

195 X. Sun, Y. Ding, B. Niu and Q. Chen, Evaluation of a composite nanomaterial consist of gold nanoparticles and graphene-carbon nitride as capillary electrochromatography stationary phase for enantioseparation, *Microchem. J.*, 2021, **169**, 1–8.

196 Z. Jiang, J. Qu, X. Tian, X. Huo, J. Zhang, X. Guo and L. Fang, Sol-gel technique for the preparation of β-cyclodextrin gold nanoparticles as chiral stationary phase in open-tubular capillary electrochromatography, *J. Sep. Sci.*, 2019, **42**, 1948–1954.

197 L. Zhou, S. Jiang, X. Zhang, L. Fang and X. Guo, Preparation of β-cyclodextrin-gold nanoparticles modified open tubular column for capillary electrochromatographic separation of chiral drugs, *Electrophoresis*, 2018, **39**, 941–947.

198 L. Fang, P. Wang, X. Wen, X. Guo, L. Luo, J. Yu and X. Guo, Layer-by-layer self-assembly of gold nanoparticles/thiols β-cyclodextrin coating as the stationary phase for enhanced chiral differentiation in open tubular capillary electrochromatography, *Talanta*, 2017, **167**, 158–165.

199 F. Wang, W. Lv, Y. Zhang, X. Niu, X. Wu, H. Chen and X. Chen, Synthesis of spherical three-dimensional covalent organic frameworks and in-situ preparation of capillaries coated with them for capillary electrochromatographic separation, *J. Chromatogr. A*, 2022, **1681**, 1–9.

200 R. Liu, G. Yi, B. Ji, X. Liu, Y. Gui, Z. Xia and Q. Fu, Metal-organic frameworks-based immobilized enzyme microreactors integrated with capillary electrochromatography for high-efficiency enzyme assay, *Anal. Chem.*, 2022, **94**, 6540–6547.

201 Y. Wang, D. I. Adeoye, E. O. Ogunkunle, I. Wei, R. T. Filla and M. G. Roper, Affinity capillary electrophoresis: a critical review of the literature from 2018 to 2020, *Anal. Chem.*, 2021, **93**, 295–310.

202 L. Yang, X. Zhao, Y. Chai, C. Li, Y. Zhang, L. Chen, J. Ye and Q. Chu, Preparation and evaluation of chiral open-tubular columns supported with zeolite silica nanoparticles and single/dual chiral selectors using capillary electrochromatography with amperometric detection, *J. Chromatogr. A*, 2021, **1651**, 1–5.

203 X. Yang, X. Sun, Z. Feng, Y. Du, J. Chen, X. Ma and X. Li, Open-tubular capillary electrochromatography with β-cyclodextrin-functionalized magnetic nanoparticles as stationary phase for enantioseparation of dansylated amino acids, *Microchim. Acta*, 2019, 1–8.

204 X. Sun, Y. Du, S. Zhao, Z. Huang and Z. Feng, Enantioseparation of propranolol, amlodipine and metoprolol by electrochromatography using an open tubular capillary modified with β-cyclodextrin and poly(glycidyl methacrylate) nanoparticles, *Microchim. Acta*, 2019, **186**, 1–7.

205 X. Sun, Y. Tao, Y. Du, W. Ding, C. Chen and X. Ma, Metal organic framework HKUST-1 modified with carboxymethyl-β-cyclodextrin for use in improved open tubular capillary electrochromatographic enantioseparation of five basic drugs, *Microchim. Acta*, 2019, **186**, 1–8.

206 Z. Li, Z. Mao, W. Zhou and Z. Chen, γ-Cyclodextrin metal-organic framework supported by polydopamine as stationary phases for electrochromatographic enantioseparation, *Talanta*, 2020, **218**, 1–7.

207 T. Wang, Y. Cheng, Y. Zhang, J. Zha, J. Ye, Q. Chu and G. Cheng, β-cyclodextrin modified quantum dots as pseudo-stationary phase for direct enantioseparation based on capillary electrophoresis with laser-induced fluorescence detection, *Talanta*, 2020, **210**, 1–8.

